

Efficient First-order Methods for Convex Optimization with Strongly Convex Function Constraints

Zhenwei Lin* Qi Deng †

December 22, 2022

Abstract

Convex function constrained optimization has received growing research interests lately. For a special convex problem which has strongly convex function constraints, we develop a new accelerated primal-dual first-order method that obtains an $\mathcal{O}(1/\sqrt{\varepsilon})$ complexity bound, improving the $\mathcal{O}(1/\varepsilon)$ result for the state-of-the-art first-order methods. The key ingredient to our development is some novel techniques to progressively estimate the strong convexity of the Lagrangian function, which enables adaptive step-size selection and faster convergence performance. In addition, we show that the complexity is further improvable in terms of the dependence on some problem parameter, via a restart scheme that calls the accelerated method repeatedly. As an application, we consider sparsity-inducing constrained optimization which has a separable convex objective and a strongly convex loss constraint. In addition to achieving fast convergence, we show that the restarted method can effectively identify the sparsity pattern (active-set) of the optimal solution in finite steps. To the best of our knowledge, this is the first active-set identification result for sparsity-inducing constrained optimization.

1 Introduction

In this paper, we focus on the following convex inequality-constrained problem:

$$\begin{aligned} \min_{\mathbf{x} \in \mathbb{R}^n} \quad & f(\mathbf{x}) \\ \text{s.t.} \quad & g_i(\mathbf{x}) \leq 0, \quad 1 \leq i \leq m, \end{aligned} \tag{1}$$

where $f : \mathbb{R}^n \rightarrow \mathbb{R}$ is a convex continuous function and $g_i : \mathbb{R}^n \rightarrow \mathbb{R}$ is a continuously differentiable and strongly convex function, for $i = 1, 2, \dots, m$. A motivating application of our methods is the constrained Lasso-type problem which minimizes a sparsity-inducing regularizer while explicitly requiring the data fitting error under control:

$$\min_{\mathbf{x} \in \mathbb{R}^n} \|\mathbf{x}\|_1 \quad \text{s.t.} \quad g(\mathbf{x}) \leq 0, \tag{2}$$

where $g(\cdot)$ is a strongly convex loss function. Compared with the standard Lasso problem [30]

$$\min_{\mathbf{x} \in \mathbb{R}^n} g(\mathbf{x}) + \lambda \|\mathbf{x}\|_1, \tag{3}$$

the constrained problem (2) appears to be far more challenging due to the complicated nonlinear constraint.

There is a vast literature on convex function constrained optimization lately which focus on the algorithm efficiency guarantee in a finite iteration number ([19, 18, 35, 33, 2, 1, 23, 20, 34, 31, 25]). When both $f(\mathbf{x})$ and $g_i(\mathbf{x})$ are convex and smooth (or composite), the best complexity result is $\mathcal{O}(1/\varepsilon)$, for guaranteeing an ε -error in optimality gap and constraint violation. Popular methods include Augmented Lagrangian methods [19, 34], level-set methods [23], penalty methods [18]. When the objective is strongly convex,

*zhenweilin@163.sufe.edu.cn, Shanghai University of Finance and Economics

†qideng@sufe.edu.cn, Shanghai University of Finance and Economics

the complexity can be further improved to $\mathcal{O}(1/\sqrt{\varepsilon})$. Notice that all of these methods involve first-order methods, such as Nesterov’s accelerated gradient method, to solve certain strongly convex and proximal inner problems. In [5], the authors proposed a level constrained proximal gradient (LCPG) which can further reduce the complexity in evaluating function and gradient values. Particularly, when $f(\mathbf{x})$ is strongly convex, the LCPG method only needs an $\mathcal{O}(\log(1/\varepsilon))$ function/gradient evaluations. However, LCPG still requires to solve a structured strongly convex constrained subproblem to pre-specified accuracy.

While a great progress has been made in developing fast nested algorithms, it is often more favorable to use single-loop algorithms, thanks to their simplicity and ease in implementation. For example, Xu [33] developed a first-order algorithm based on linearizing the augmented Lagrangian function, obtaining a convergence rate of $\mathcal{O}(1/\varepsilon)$. Viewing (1) as a special case of min-max problem:

$$\min_{\mathbf{x} \in \mathbb{R}^n} \max_{\mathbf{y} \in \mathbb{R}^m} \mathcal{L}(\mathbf{x}, \mathbf{y}) := f(\mathbf{x}) + \sum_{i=1}^m y_i g_i(\mathbf{x}), \quad \text{s.t. } y_i \geq 0, \quad i = 1, 2, \dots, m, \quad \text{eq:min-max (4)}$$

Hamedani and Aybat [11] proposed to solve (1) by an accelerated primal-dual method (APD), which generalizes the celebrated primal-dual hybrid gradient method [8] initially developed for saddle point optimization with bilinear coupling term. Under mild conditions, APD achieves the best $\mathcal{O}(1/\varepsilon)$ convergence rate for general convex constrained problem and the further improve the rate to $\mathcal{O}(1/\sqrt{\varepsilon})$ when $f(\mathbf{x})$ is strongly convex. Boob et al. [6] proposed a unified constrained extrapolation method which can be applied to both deterministic or stochastic constrained optimization problems.

In spite of these recent progress, to the best of our knowledge, there still does not exist an optimal method for solving strongly convex constrained problem (1). By directly applying those aforementioned algorithms, the obtained $\mathcal{O}(1/\varepsilon)$ complexity is substantially worse than the optimal rate $\mathcal{O}(1/\sqrt{\varepsilon})$. This is somewhat unsatisfactory, as the strong convexity of $g(\mathbf{x})$ appears to be of no use to enable further acceleration. It is natural to ask the following question:

Can we further improve the convergence rate of first-order methods for solving strongly convex constrained problem (1)?

To answer this question, we take a closer look at the Lagrangian function in (4). It can be seen that the strong convexity of $\mathcal{L}(\cdot, \mathbf{y})$ with respect to \mathbf{x} is closely related to the scale of dual sequence \mathbf{y} , which keeps changing over the algorithm iterations. When strong convexity with respect to \mathbf{x} does not hold uniformly, there is a substantial challenge to achieve the known optimal rate $\mathcal{O}(1/\sqrt{\varepsilon})$ for strongly-convex-concave optimization ([24]). To overcome such difficulty, we make a mild assumption that the unconstrained minimizer of $f(\mathbf{x})$ is infeasible, which ensures strict separation between origin and the subdifferential at optimal solution $\partial f(\mathbf{x}^*)$. By exploiting structures of such objective and the strongly convex constraints, we develop new lower bounds for the norm of optimal dual variables $\|\mathbf{y}^*\|$. This bound is valid under mild assumptions and is easily computable using the generated primal and dual sequence $\{\mathbf{x}_k, \mathbf{y}_k\}$. More importantly, this bound allows us to effectively exploit the strong convexity of the Lagrangian function and use more aggressive stepsize parameters. Consequently, we are able to develop novel adaptive accelerated methods that have substantially better complexity bounds than the $\mathcal{O}(1/\varepsilon)$ complexity of APD.

Comparison with Frank-Wolfe It should be noted that strongly convex function constraint in (1) is a special case of strongly convex set constraint. See [15] for the proof. Over the strongly convex set, it has been shown that Frank-Wolfe Algorithm (FW) can obtain convergence rates substantially better than the standard $\mathcal{O}(1/\varepsilon)$ rate. Under the bounded gradient assumption, [9, 22] shows that FW obtains linear convergence over a strongly convex set. [10] shows that FW obtains an $\mathcal{O}(1/\sqrt{\varepsilon})$ rate when the gradient is the order of square root of function value gap. We refer to the survey [7] for more recent progress. However, despite the attractive convergence property, FW has some limitation for solving (1). Specifically, FW involves a sequence of linear optimization problems over the iterations. While linear optimization over certain strongly convex sets, such as ℓ_p -ball, admits a closed-form solution, there is unfortunately no efficient routine to handle general function constraints studied in this paper.

Sparsity identification Besides concerning about the algorithm efficiency for solving (2), it is often desired to show the active set (or sparsity) identification, namely, the nonzero patterns of the optimal solution \mathbf{x}^* can be identified by the solution sequence $\{\mathbf{x}^k\}$ in a finite number of iterations. After that, it is possible to leverage the low-dimensional structure for further acceleration [14]. Identifying the embedded solution structure, in a wider context, has been known as the manifold identification problem, studied in constrained optimization [32] and nonsmooth optimization [12]. For the regularized problem (3), it has been known that proximal gradient and some other first-order methods (e.g. [14]) enjoy the finite active-set identification property, and a regularized dual-averaging method can identify the sparsity pattern with high probability in stochastic setting [21]. Under a mild non-degenerated condition, [26] introduced the "active set complexity", which is defined as the number of iterations required before an algorithm is guaranteed to have reached the optimal manifold, and they proved the proximal gradient method with constant step-size can identify the optimal manifold in a finite number of iterations. For the constrained problem (2), it is desirable to know whether one can show the same effectiveness of first-order methods in sparsity identification.

1.1 Contributions

In this paper, we address the aforementioned theoretical questions about the strongly convex constrained optimization and the application on sparse optimization. Our contributions are summarized as follows.

First, for the strongly convex constrained problem (1), we develop a new accelerated primal-dual algorithm with progressive strong convexity estimation (APDPro). APDPro employs a novel strategy to estimate the lower bound of the dual variables, which leads to a strictly positive and gradually refined estimated strong convexity modulus of $\mathcal{L}(\cdot, \mathbf{y})$. Moreover, with additional new cut constraints on the dual update, APDPro is able to separate the dual search space from the origin, which is critical for maintaining the desired strong convexity over the entire solution path. With these two important ingredients, APDPro exhibits an $\mathcal{O}(\|\mathbf{x}_0 - \mathbf{x}^*\| + D_Y)/\sqrt{\varepsilon}$ complexity bound to obtain an ε -error on the function value gap and constraint violation, where D_Y is an upper-bound of $\|\mathbf{y}_0 - \mathbf{y}^*\|$. Moreover, we show that for the last iterate to have an ε error (i.e. $\|\mathbf{x}_K - \mathbf{x}^*\|^2 \leq \varepsilon$), APDPro requires a total iteration of $\mathcal{O}(\|\mathbf{x}_0 - \mathbf{x}^*\| + \|\mathbf{y}_0 - \mathbf{y}^*\|)/\sqrt{\varepsilon}$. Both complexity results appear to be new in the literature for strongly convex constrained optimization

Second, we present a new restart algorithm (rAPDPro) which calls APDPro repeatedly with the input parameters properly changing over time. Different from APDPro, rAPDPro dynamically adjust the iteration number of APDPro in each epoch based on the progressive strong convexity estimation. We show that rAPDPro exhibits a complexity of $\mathcal{O}(\log(D_X/\sqrt{\varepsilon}) + D_Y/\sqrt{\varepsilon})$ to ensure ε -error in the last iterate convergence where D_X is the estimated diameter of the primal feasible domain. While it is difficult to improve the overall $\mathcal{O}(1/\sqrt{\varepsilon})$ bound, rAPDPro appears to be more advantageous when D_X and D_Y are the same order of $\|\mathbf{x}_0 - \mathbf{x}^*\|$ and $\|\mathbf{y}_0 - \mathbf{y}^*\|$, respectively, and $D_X \gg D_Y$. In addition, we show that a similar restart strategy can further accelerate the standard APD that does not utilize the strong convexity assumption. The resulting multistage-accelerated primal dual method (msAPD) obtains a comparable $\mathcal{O}(1/\sqrt{\varepsilon})$ complexity of APDPro without introducing additional cut constraint.

Third, we apply our proposed methods to solve the sparse learning problem (2). In view of the theoretical analysis, all our methods converge at an $\mathcal{O}(1/\sqrt{\varepsilon})$ rate, which is substantially better than the rates of state-of-the-art first-order algorithms. Moreover, we conduct a new analysis to show that the restart algorithm rAPDPro has the favorable feature of identifying the optimal sparsity pattern. Note that such active-set/manifold identification is substantially more challenging to prove due to the coupling of dual variables and constraint functions. To establish the desired property, we develop asymptotic convergence of the dual sequence to the optimal solution, which can be of independent interests.

1.2 Outline

This paper proceeds as follows. In Section 2, we set notations and make some basic assumptions for the later theoretical development. Section 3 presents the APDPro algorithm and develop its stepsize rule and complexity rate. Section 4 presents the restart APDPro algorithm with both asymptotic and nonasymptotic convergence analysis. Section 5 presents the multistage algorithm msAPD which does not rely on adding dual cut constraint. Section 6 apply our proposed method for sparsity-inducing constrained optimization,

and show the sparsity identification result for rAPDPro. In Section 7, we conduct numerical results to examine the convergence and sparsity identification performance of our proposed algorithms. Finally, we draw conclusion in Section 8. All the missing proofs are provided in the appendix sections.

2 Preliminaries

We use bold letters such as $\mathbf{x}, \mathbf{y}, \mathbf{z}$ to represent vectors. Suppose $\mathbf{x} \in \mathbb{R}^n$, we use $\|\mathbf{x}\|_q = (\sum_{i=1}^n |\mathbf{x}_{(i)}|^q)^{1/q}$ to represent the l_q -norm, where $\mathbf{x}_{(i)}$ denotes the i -th element of \mathbf{x} . For brevity, $\|\mathbf{x}\|$ stands for l_2 -norm. For a matrix A , we denote the matrix norm induced by 2-norm as $\|A\| = \sup_{\|\mathbf{x}\| \leq 1} \|A\mathbf{x}\|$. We also use $\mathcal{B}(\mathbf{x}, r)$ to denote a closed ball centered at \mathbf{x} with radius $r > 0$, i.e., $\mathcal{B}(\mathbf{x}, r) = \{\mathbf{y} \mid \|\mathbf{y} - \mathbf{x}\| \leq r\}$. The normal cone of \mathcal{X} at \mathbf{u} is denoted as $\mathcal{N}_{\mathcal{X}}(\mathbf{u}) := \{\mathbf{v} \mid \langle \mathbf{v}, \mathbf{x} - \mathbf{u} \rangle \leq 0, \forall \mathbf{x} \in \mathcal{X}\}$.

For brevity, we write $G(\mathbf{x}) = [g_1(\mathbf{x}), \dots, g_m(\mathbf{x})]^T$ and denote the set of feasible solutions by $\mathcal{X}_G = \{\mathbf{x} \mid g_i(\mathbf{x}) \leq 0, \forall i \in [m]\}$. We assume each $g_i(\mathbf{x})$ is a strongly convex function with modulus $\mu_i > 0$, and denote $\boldsymbol{\mu} := [\mu_1, \dots, \mu_m]^T$. Let $[m] := \{1, \dots, m\}$ for integer m . Denote $\underline{\mu} := \min_{j \in [m]} \{\mu_j\}$, and $\bar{\mu} := \max_{j \in [m]} \{\mu_j\}$. We denote the vector of elements 0 by $\mathbf{0}$.

We state some basic results in nonlinear programming. Recall that the Lagrangian function of problem (1) is given by $\mathcal{L}(\mathbf{x}, \mathbf{y}) := f(\mathbf{x}) + \langle \mathbf{y}, G(\mathbf{x}) \rangle$ where $\mathbf{y} \in \mathbb{R}_+^m$. We say that \mathbf{x}^* satisfies the *KKT condition* if there exist a Lagrangian multiplier vector $\mathbf{y}^* \in \mathbb{R}^m$ such that

$$\mathbf{0} \in \partial \mathcal{L}(\mathbf{x}^*, \mathbf{y}^*), \quad \mathbf{0} \leq \mathbf{y}^* \perp -G(\mathbf{x}^*) \geq \mathbf{0}. \quad \text{eq:KKT-cond} \tag{5}$$

The KKT condition is necessary for optimality when a constraint qualification holds at \mathbf{x}^* . Typically, we assume the following Slater's constraint qualification holds, which, according to standard convex optimization theory (see [4]), guarantees that an optimal solution is also a KKT point.

Assumption 1 (Slater's condition). *There exists a strictly feasible point $\tilde{\mathbf{x}} \in \mathbb{R}^n$ such that $G(\tilde{\mathbf{x}}) < \mathbf{0}$.*

We require the following assumption to circumvent any trivial solution.

Assumption 2. *The minimizer of function $f(\mathbf{x})$ is infeasible for problem (1), namely, for any $\mathbf{x}_0^* \in \text{argmin}_{\mathbf{x}} f(\mathbf{x})$, there exists an $i \in [m]$ such that $g_i(\mathbf{x}_0^*) > 0$.*

In view of Assumption 2, the function constraint requires us to find a solution different from the minimizer of the objective $f(\mathbf{x})$. Note that Assumption 2 is indeed a mild condition and is easily verifiable. Particularly, when $f(\mathbf{x})$ is a sparsity-inducing regularizer, we have the unconstrained minimizer $\mathbf{x}_0^* = \mathbf{0}$. Assumption 2 implies that \mathbf{x}_0^* is infeasible for problem (1). On the other hand, if Assumption 2 fails, we immediately conclude that $\mathbf{x}_0^* = \mathbf{0}$ is the optimal solution. Next, we give several useful properties about the optimal solutions of problem (1). The following result is a simple extension of Proposition 2 in [6]. We provide the proof for completeness.

Proposition 1. *Suppose Assumption 1 holds, then the optimal dual variable of problem (1) located in set $\mathcal{Y} := \{\mathbf{y} \in \mathbb{R}_+^m \mid \|\mathbf{y}\| \leq \bar{c}\}$, where $\bar{c} := \frac{f(\tilde{\mathbf{x}}) - \min_{\mathbf{x}} f(\mathbf{x})}{\min_{i \in [m]} \{-g_i(\tilde{\mathbf{x}})\}}$.*

Proof. Let $\mathbf{x}^*, \mathbf{y}^*$ be the primal and dual optimal solution. For any $\mathbf{x} \in \mathcal{X}_G$, we have

$$f(\mathbf{x}) + \langle \mathbf{y}^*, G(\mathbf{x}) \rangle \geq f(\mathbf{x}^*) + \langle \mathbf{y}^*, G(\mathbf{x}^*) \rangle = f(\mathbf{x}^*),$$

where the equality is from the complementary slackness condition. In view of the above result and the Slater's condition (i.e. $G(\tilde{\mathbf{x}}) < \mathbf{0}$), we have

$$\begin{aligned} f(\tilde{\mathbf{x}}) &\geq f(\tilde{\mathbf{x}}) + \langle \mathbf{y}^*, G(\tilde{\mathbf{x}}) \rangle \geq f(\mathbf{x}^*), \\ \Rightarrow \|\mathbf{y}^*\|_1 \min_{i \in [m]} \{-g_i(\tilde{\mathbf{x}})\} &\leq -\langle \mathbf{y}^*, G(\tilde{\mathbf{x}}) \rangle \leq f(\tilde{\mathbf{x}}) - f(\mathbf{x}^*), \\ \Rightarrow \|\mathbf{y}^*\| &\leq \|\mathbf{y}^*\|_1 \leq \frac{f(\tilde{\mathbf{x}}) - f(\mathbf{x}^*)}{\min_{i \in [m]} \{-g_i(\tilde{\mathbf{x}})\}} \leq \bar{c}, \end{aligned} \quad \text{eq:tighter} \tag{6}$$

where the last inequality is by $f(\mathbf{x}^*) \geq f(\mathbf{x}_0^*)$, since $\mathbf{x}_0^* \in \text{argmin}_{\mathbf{x} \in \mathbb{R}^n} f(\mathbf{x})$. Hence, we complete our proof. \square

Proposition 2. *When Assumption 2 holds, the optimal solution \mathbf{x}^* of problem (1) is unique. Let $\mathcal{Y}^* := \operatorname{argmax}_{\mathbf{y}} \mathcal{L}(\mathbf{x}^*, \mathbf{y})$ denote the set containing all the optimal dual variables, then \mathcal{Y}^* is a convex set.*

Proof. We prove the uniqueness property by contradiction. Suppose there exist $(\mathbf{x}^*, \mathbf{y}^*)$, $(\tilde{\mathbf{x}}^*, \tilde{\mathbf{y}}^*)$ satisfying the KKT condition, then we have $\mathcal{L}(\mathbf{x}^*, \mathbf{y}^*) = f(\mathbf{x}^*) = f(\tilde{\mathbf{x}}^*) = \mathcal{L}(\tilde{\mathbf{x}}^*, \tilde{\mathbf{y}}^*)$. For $\mathcal{L}(\mathbf{x}^*, \tilde{\mathbf{y}}^*) = f(\mathbf{x}^*) + \langle \tilde{\mathbf{y}}^*, G(\mathbf{x}^*) \rangle$, we have

$$\mathcal{L}(\tilde{\mathbf{x}}^*, \tilde{\mathbf{y}}^*) \leq \mathcal{L}(\mathbf{x}^*, \tilde{\mathbf{y}}^*) \leq \mathcal{L}(\mathbf{x}^*, \mathbf{y}^*).$$

Hence, we must have $\mathcal{L}(\tilde{\mathbf{x}}^*, \tilde{\mathbf{y}}^*) = \mathcal{L}(\mathbf{x}^*, \tilde{\mathbf{y}}^*)$. However, as we argued that $\tilde{\mathbf{y}}^* \neq \mathbf{0}$ in Assumption 2, the strongly convex function $\mathcal{L}(\cdot, \tilde{\mathbf{y}}^*)$ has a unique optimizer. Therefore, we conclude that $\mathbf{x}^* = \tilde{\mathbf{x}}^*$.

Next, we show that the set of optimal dual variables for problem (1) is convex. Suppose that there exist two optimal dual variables \mathbf{y}_1^* and \mathbf{y}_2^* for \mathbf{x}^* , both satisfying the KKT condition, then we have $\langle \mathbf{y}_1^*, G(\mathbf{x}^*) \rangle = \langle \mathbf{y}_2^*, G(\mathbf{x}^*) \rangle = 0$. This implies that any linear combination of \mathbf{y}_1^* and \mathbf{y}_2^* satisfy KKT condition, i.e., $\langle a\mathbf{y}_1^* + b\mathbf{y}_2^*, G(\mathbf{x}^*) \rangle = 0, \forall a, b$. From Proposition 1, we know any optimal dual variable falls into a compact convex set \mathcal{Y} , which completes the proof. \square

In view of Assumption 2, Proposition 2, and closeness of the subdifferential set of proper convex functions (Theorem 3.9 [3]), we derive a subdifferential separation result which will be used repeatedly in our algorithm development. Specifically, for the optimal solution \mathbf{x}^* , we have

$$\mathbf{dist}(\partial f(\mathbf{x}^*), \mathbf{0}) \geq r > 0, \tag{7} \text{eq:subdiff_lb}$$

for some real value r , where $\mathbf{dist}(\partial f(\mathbf{x}^*), \mathbf{0}) := \min_{\xi \in \partial f(\mathbf{x}^*)} \|\xi\|$. We give some important examples for which the lower bound r can be estimated. Suppose $f(\mathbf{x})$ is a Lasso regularizer, i.e., $f(\mathbf{x}) = \|\mathbf{x}\|_1$, then $r = 1$ satisfies (7). More general, consider the group Lasso regularizer, i.e., $f(\mathbf{x}) = \sum_{i=1}^B p_i \|\mathbf{x}_{(i)}\|$, where $\mathbf{x}_{(i)} \in \mathbb{R}^{b_i}$ and $\sum_{i=1}^B b_i = n$, B is the number of blocks, then $r = \min_i p_i$ when $\mathbf{x}^* \neq \mathbf{0}$. Another example is when $f(\mathbf{x})$ is a linear function, namely, $\mathbf{c}^T \mathbf{x}$, where $\mathbf{c} \in \mathbb{R}^n$, then we have $r = \|\mathbf{c}\|$.

Remark 1. Condition (7) is similar to the bounded gradient assumption that has been used for accelerating the convergence of Frank-Wolfe algorithm. Specifically, assuming that $f(\mathbf{x})$ is smooth and its gradient is uniformly bounded by $\|\nabla f(\mathbf{x})\| > c > 0$ for any feasible solution \mathbf{x} , [9, 22] further improve the convergence rate of Frank-Wolfe algorithm from $\mathcal{O}(1/\varepsilon)$ to $\mathcal{O}(\log(1/\varepsilon))$. Nevertheless, the uniform bounded gradient assumption appears to be stronger than ours, as we only impose the lower boundedness assumption on the optimal solution \mathbf{x}^* and allow the objective to be nondifferentiable.

Proposition 3. *Under Assumptions 1 and 2, the feasible set of \mathbf{x} is bounded, i.e., $\max_{\mathbf{x}_1, \mathbf{x}_2 \in \mathcal{X}_G} \|\mathbf{x}_1 - \mathbf{x}_2\| \leq \min_{i \in [m]} 2\sqrt{\frac{-2g_i(\mathbf{x}_i^*)}{\mu_i}}$, where $\mathbf{x}_i^* = \operatorname{argmin}_{\mathbf{x} \in \mathbb{R}^n} g_i(\mathbf{x})$. Let $\mathcal{X} := \mathcal{B}(\tilde{\mathbf{x}}, \min_{i \in [m]} 2\sqrt{\frac{-2g_i(\mathbf{x}_i^*)}{\mu_i}} + \zeta)$, where ζ is a positive constant, then $\mathbf{x}^* \in \operatorname{int} \mathcal{X}$.*

Proof. From the strong convexity of $g_i(\mathbf{x})$, we have $g_i(\mathbf{x}) \geq g_i(\mathbf{x}_i^*) + \frac{\mu_i}{2} \|\mathbf{x} - \mathbf{x}_i^*\|^2$, for any $\mathbf{x} \in \mathcal{X}_G$. Then we have

$$\|\mathbf{x} - \mathbf{x}_i^*\|^2 \leq (g_i(\mathbf{x}) - g_i(\mathbf{x}_i^*)) \frac{2}{\mu_i} \leq \frac{-2g_i(\mathbf{x}_i^*)}{\mu_i}.$$

In view of the triangle inequality and the above result, for any $\mathbf{x}_1, \mathbf{x}_2 \in \mathcal{X}_G$, we have

$$\|\mathbf{x}_1 - \mathbf{x}_2\| \leq \|\mathbf{x}_1 - \mathbf{x}_i^*\| + \|\mathbf{x}_2 - \mathbf{x}_i^*\| \leq 2\sqrt{\frac{-2g_i(\mathbf{x}_i^*)}{\mu_i}}.$$

Hence, $\mathbf{x}^* \in \mathcal{B}(\tilde{\mathbf{x}}, \min_{i \in [m]} 2\sqrt{\frac{-2g_i(\mathbf{x}_i^*)}{\mu_i}})$. Combine the fact ζ is a positive constant, then we have $\mathbf{x}^* \in \operatorname{int} \mathcal{X}$. \square

Assumption 3. *There exist $L_X, L_G > 0$ such that*

$$\|\nabla G(\mathbf{x}) - \nabla G(\bar{\mathbf{x}})\| \leq L_X \|\mathbf{x} - \bar{\mathbf{x}}\|, \quad \forall \mathbf{x}, \bar{\mathbf{x}} \in \mathcal{X}, \tag{8} \text{eq:lipshitz_x}$$

$$\|G(\mathbf{x}) - G(\bar{\mathbf{x}})\| \leq L_G \|\mathbf{x} - \bar{\mathbf{x}}\|, \quad \forall \mathbf{x}, \bar{\mathbf{x}} \in \mathcal{X}, \tag{9} \text{eq:lipshitz_func}$$

where $\nabla G(\mathbf{x}) := [\nabla g_1(\mathbf{x}), \dots, \nabla g_m(\mathbf{x})] \in \mathbb{R}^{n \times m}$.

Proposition 3 and Proposition 1 guarantee that the primal and dual optimal solutions are in an enlarged bounded set \mathcal{X} and \mathcal{Y} , respectively, thereby ensuring the Lipschitzness of Lagrangian function in the domain. Combining the inequality (8) and the fact $\|\mathbf{y}\| \leq \|\mathbf{y}\|_1 \leq \bar{c}, \forall \mathbf{y} \in \mathcal{Y}$ by (6), we obtain that

$$\|\nabla G(\mathbf{x})\mathbf{y} - \nabla G(\bar{\mathbf{x}})\mathbf{y}\| \leq L_{XY}\|\mathbf{x} - \bar{\mathbf{x}}\| \quad \forall \mathbf{x}, \bar{\mathbf{x}} \in \mathcal{X}, \quad \forall \mathbf{y} \in \mathcal{Y}, \quad \text{eq:lipshitz_xy} \quad (10)$$

where $L_{XY} = \bar{c}L_X$. For set \mathcal{X} , \mathcal{Y} , we let D_X and D_Y denote their diameters, respectively, i.e., $D_X := \max_{\mathbf{x}_1, \mathbf{x}_2 \in \mathcal{X}} \|\mathbf{x}_1 - \mathbf{x}_2\|$, and $D_Y := \max_{\mathbf{y}_1, \mathbf{y}_2 \in \mathcal{Y}} \|\mathbf{y}_1 - \mathbf{y}_2\|$.

3 APD with Progressive Strong Convexity Estimation

In this section, we present the Accelerated Primal-Dual Algorithm with Progressive Strong Convexity Estimation (APDPro) to solve problem (1). In the algorithm running process, we apply a new technique to improve the estimated strong convexity modulus of the Lagrangian function. For problem (1), APDPro achieves the improved convergence rate $\mathcal{O}(1/\sqrt{\varepsilon})$ without relying on the uniform strong convexity assumption [16, 11, 24]. For notations, we denote $\text{prox}_{f, \mathcal{X}}(\mathbf{x}, \mathbf{z}, \eta) = \text{argmin}_{\hat{\mathbf{x}} \in \mathcal{X}} f(\hat{\mathbf{x}}) + \langle \mathbf{z}, \hat{\mathbf{x}} \rangle + \frac{1}{2\eta} \|\hat{\mathbf{x}} - \mathbf{x}\|^2$ as the proximal mapping associated with $f(\cdot) + \langle \mathbf{z}, \cdot \rangle$ on \mathcal{X} .

We describe the details of APDPro in Algorithm 1. The main component of APDPro contains a dual ascent step to update \mathbf{y}_k based on using the extrapolated gradient descent, and a proximal gradient descent for primal variable \mathbf{x}_k . Compared with standard accelerated primal dual method [11], APDPro has two more important steps that substantially improve the algorithm convergence. First, line 4 of Algorithm 1 provides a novel cut constraint to separate the dual sequence $\{\mathbf{y}_k\}$ from the origin, which allows us to leverage the strong convexity of the Lagrangian function and hence obtain a faster rate of convergence than APD [11]. Second, to use the strong convexity more effectively, in line 10 we perform a progressive estimation of the strong convexity by using the latest iterates \mathbf{x}_k and $\bar{\mathbf{x}}_k$. Throughout the algorithm process, we use a simple routine IMPROVE (line 13 to 16) to construct a monotonically increasing sequence $\{\rho_k\}$, which provides increasingly refined lower bounds of the strong convexity of the Lagrangian function and better cut constraints for the dual update.

Algorithm 1 Accelerated Primal-Dual Algorithm with Progressive Strong Convexity Estimation (APDPro)

Require: $\tau_0 > 0, \sigma_0 > 0, \mathbf{x}_0 \in \mathcal{X}, \mathbf{y}_0 \in \mathcal{Y}, \rho_0 \geq 0, N > 0$

- 1: **Initialize:** $(\mathbf{x}_{-1}, \mathbf{y}_{-1}) \leftarrow (\mathbf{x}_0, \mathbf{y}_0), \bar{\mathbf{x}}_0 \leftarrow \mathbf{x}_0, \sigma_{-1} \leftarrow \sigma_0, \gamma_0 \leftarrow \sigma_0/\tau_0, T_0 = 0$
 - 2: Set $\Delta_{XY} = \frac{1}{2\tau_0} D_X^2 + \frac{1}{2\sigma_0} D_Y^2$
 - 3: **for** $k = 0, 1, \dots, N$ **do**
 - 4: $\mathcal{Y}_k \leftarrow \{\mathbf{y} \in \mathbb{R}_+^m \mid \|\mathbf{y}\|_1 \cdot \underline{\mu} \geq \rho_k\} \cap \mathcal{Y}$
 - 5: Compute θ_k
 - 6: $\mathbf{z}_k \leftarrow (1 + \theta_k)G(\mathbf{x}_k) - \theta_k G(\mathbf{x}_{k-1})$
 - 7: $\mathbf{y}_{k+1} \leftarrow \text{prox}_{\mathbf{0}, \mathcal{Y}_k}(\mathbf{y}_k, -\mathbf{z}_k, \sigma_k)$
 - 8: $\mathbf{x}_{k+1} \leftarrow \text{prox}_{f, \mathcal{X}}(\mathbf{x}_k, \nabla G(\mathbf{x}_k)\mathbf{y}_{k+1}, \tau_k)$
 - 9: $t_k \leftarrow \sigma_k/\sigma_0, \bar{\mathbf{x}}_{k+1} \leftarrow (T_k \bar{\mathbf{x}}_k + t_k \mathbf{x}_{k+1})/(T_k + t_k), T_{k+1} \leftarrow T_k + t_k$
 - 10: Update $\rho_{k+1} \leftarrow \text{IMPROVE}(\mathbf{x}_k, \bar{\mathbf{x}}_k, \frac{\sigma_0 \tau_{k-1} \Delta_{XY}}{\sigma_{k-1}}, \frac{\Delta_{XY}}{T_k}, \rho_k)$
 - 11: Update γ_{k+1}, τ_{k+1} , and σ_{k+1} depended on ρ_{k+1}
 - 12: **Output:** $\mathbf{x}_{N+1}, \mathbf{y}_{N+1}$
 - 13: **procedure** IMPROVE($\mathbf{x}, \bar{\mathbf{x}}, \beta, \bar{\beta}, \rho_{\text{old}}$)
 - 14: Compute $\rho = \underline{\mu} \cdot \max \left\{ r [\|\nabla G(\mathbf{x})\| + L_X \sqrt{2\beta}]^{-1}, \left[\frac{L_X}{r} \sqrt{\frac{\bar{\beta}}{2\underline{\mu}}} + \sqrt{\frac{L_X^2 \bar{\beta}}{2\underline{\mu} r^2} + \frac{\|\nabla G(\bar{\mathbf{x}})\|}{r}} \right]^{-2} \right\}$
 - 15: Set $\rho_{\text{new}} = \max\{\rho_{\text{old}}, \rho\}$
 - 16: **return** ρ_{new}
-

The IMPROVE step In order to estimate strong convexity of the Lagrangian function, we rely on the subdifferential separation (i.e. eq.(7)) to bound the dual variables. From the first-order optimality condition

in minimizing $\mathcal{L}(\mathbf{x}, \mathbf{y}^*)$ and the fact that $\mathbf{x}^* \in \mathbf{int} \mathcal{X}$ (i.e. Proposition 3), we have

$$\mathbf{0} \in \partial f(\mathbf{x}^*) + \nabla G(\mathbf{x}^*)\mathbf{y}^* + N_{\mathcal{X}}(\mathbf{x}^*) = \partial f(\mathbf{x}^*) + \nabla G(\mathbf{x}^*)\mathbf{y}^*.$$

It follows from (7) that

$$r \leq \|\nabla G(\mathbf{x}^*)\mathbf{y}^*\| \leq \|\nabla G(\mathbf{x}^*)\| \cdot \|\mathbf{y}^*\| \leq \|\mathbf{y}^*\|_1 \|\nabla G(\mathbf{x}^*)\|, \quad \text{eq:r-lower} \quad (11)$$

where the last inequality use the fact that $\|\cdot\| \leq \|\cdot\|_1$. Note that the bound $\|\mathbf{y}^*\|_1 \geq \frac{r}{\|\nabla G(\mathbf{x}^*)\|}$ can not be readily used in the algorithm implementation because \mathbf{x}^* is generally unknown. To resolve this issue, we develop more concrete dual lower bounds by using the generated solution $\hat{\mathbf{x}}$ in the proximity \mathbf{x}^* . As we will show in the analysis, APDPro keeps track of two primal sequences $\{\mathbf{x}_k\}$ and $\{\bar{\mathbf{x}}_k\}$, for which we can establish bounds on $\|\mathbf{x}_k - \mathbf{x}^*\|^2$ and $\frac{(\mathbf{y}^*)^T \boldsymbol{\mu}}{2} \|\hat{\mathbf{x}} - \mathbf{x}^*\|^2$, respectively. This drives us to develop the following lower bound property.

Proposition 4. *Suppose Assumption 3 holds. Let $\mathbf{y}^* \in \mathcal{Y}^*$ be a dual optimal solution.*

1. *Suppose that $\frac{1}{2} \|\hat{\mathbf{x}} - \mathbf{x}^*\|^2 \leq \beta$, then we have*

$$\|\mathbf{y}^*\|_1 \geq h_1(\hat{\mathbf{x}}, \beta) := r [\|\nabla G(\hat{\mathbf{x}})\| + L_X \sqrt{2\beta}]^{-1}. \quad \text{eq:y-lb-1} \quad (12)$$

2. *Suppose $\frac{(\mathbf{y}^*)^T \boldsymbol{\mu}}{2} \|\hat{\mathbf{x}} - \mathbf{x}^*\|^2 \leq \beta$, then we have*

$$\|\mathbf{y}^*\|_1 \geq h_2(\hat{\mathbf{x}}, \beta) := \left[\frac{L_X}{r} \sqrt{\frac{\beta}{2\boldsymbol{\mu}}} + \sqrt{\frac{L_X^2 \beta}{2\boldsymbol{\mu} r^2} + \frac{\|\nabla G(\hat{\mathbf{x}})\|}{r}} \right]^{-2}. \quad \text{eq:y-lb-2} \quad (13)$$

Proof. Moreover, using the triangle inequality and (8), we have

$$\|\nabla G(\mathbf{x}^*)\| - \|\nabla G(\hat{\mathbf{x}})\| \leq \|\nabla G(\mathbf{x}^*) - \nabla G(\hat{\mathbf{x}})\| \leq L_X \|\hat{\mathbf{x}} - \mathbf{x}^*\|.$$

Combining the above inequality and (11), we obtain

$$\frac{r}{\|\mathbf{y}^*\|_1} \leq L_X \|\hat{\mathbf{x}} - \mathbf{x}^*\| + \|\nabla G(\hat{\mathbf{x}})\|. \quad \text{eq:mid-04} \quad (14)$$

Next we develop more specific lower bounds on $\|\mathbf{y}^*\|_1$. 1). Inequality (12) can be easily verified since we have $\|\hat{\mathbf{x}} - \mathbf{x}^*\| \leq \sqrt{2\beta}$. 2). Suppose $\frac{(\mathbf{y}^*)^T \boldsymbol{\mu}}{2} \|\hat{\mathbf{x}} - \mathbf{x}^*\|^2 \leq \beta$, then together with (14) we have

$$\frac{r}{\|\mathbf{y}^*\|_1} \leq L_X \sqrt{\frac{2\beta}{(\mathbf{y}^*)^T \boldsymbol{\mu}}} + \|\nabla G(\hat{\mathbf{x}})\| \leq L_X \sqrt{\frac{2\beta}{\boldsymbol{\mu} \|\mathbf{y}^*\|_1}} + \|\nabla G(\hat{\mathbf{x}})\|.$$

Note that the above inequality can be expressed as $at^2 - bt - c \leq 0$ with $t = \|\mathbf{y}^*\|_1^{-1/2}$, $a = r$, $b = L_X \sqrt{\frac{2\beta}{\boldsymbol{\mu}}}$ and $c = \|\nabla G(\hat{\mathbf{x}})\|$. Standard analysis implies that $t \leq \frac{b + \sqrt{b^2 + 4ac}}{2a}$, which gives the desired bound (13). \square

Our next goal is to conduct the convergence analysis for APDPro, which can be divided into two parts. First, under the two preconditions (15) and (16), we present the convergence conclusion for primal-dual gap and optimality gap of problem (1) (see Theorem 1). Next, we derived the convergence rate of APDPro for a specific step-size selection (see Corollary 1).

Theorem 1. *Suppose that for any $\mathbf{y}^* \in \mathcal{Y}^*$, we have $(\mathbf{y}^*)^T \boldsymbol{\mu} \geq \rho_0$, and there exists a $\delta > 0$ such that the sequence $\{\tau_k, \sigma_k, t_k\}_{k \geq 0}$ satisfies*

$$t_{k+1}(\tau_{k+1}^{-1} - \rho_{k+1}) \leq t_k \tau_k^{-1}, \quad t_{k+1} \sigma_{k+1}^{-1} \leq t_k \sigma_k^{-1}, \quad t_{k+1} \theta_{k+1} = t_k, \quad \text{eq:param-01} \quad (15)$$

$$L_{XY} + L_G^2 \sigma_k / \delta \leq \tau_k^{-1}, \quad \theta_k \delta / \sigma_{k-1} \leq \sigma_k^{-1}. \quad \text{eq:param-03} \quad (16)$$

Then, the set \mathcal{Y}_k is nonempty and $\mathcal{Y}^ \subseteq \mathcal{Y}_k$. Moreover, the sequence $\{\bar{\mathbf{x}}_k, \mathbf{x}_k, \bar{\mathbf{y}}_k\}_{k \geq 0}$ generated by APDPro satisfies*

$$\frac{t_{K-1} \tau_{K-1}^{-1}}{2T_K} \|\mathbf{x}^* - \mathbf{x}_K\|^2 + \mathcal{L}(\bar{\mathbf{x}}_K, \mathbf{y}^*) - \mathcal{L}(\mathbf{x}^*, \bar{\mathbf{y}}_K) \leq \frac{1}{T_K} \Delta(\mathbf{x}^*, \mathbf{y}^*), \quad \text{eq:apd_primal_dual_converge} \quad (17)$$

where $\bar{\mathbf{y}}_K = T_K^{-1} \sum_{s=0}^{K-1} t_s \mathbf{y}_s$, and $\Delta(\mathbf{x}^*, \mathbf{y}^*)$ is $(\mathbf{x}^*, \mathbf{y}^*)$ for function $\Delta(\mathbf{x}, \mathbf{y}) = \frac{1}{2\tau_0} \|\mathbf{x} - \mathbf{x}_0\|^2 + \frac{1}{2\sigma_0} \|\mathbf{y} - \mathbf{y}_0\|^2$.

Next, we specify the step-size selection in Lemma 1 and develop more concrete complexity result in Corollary 1.

Lemma 1. Let $\hat{\rho}_{k+1} := \frac{1}{k+1} \sqrt{\hat{\rho}_k^2 k^2 + (3\rho_{k+1} \hat{\rho}_k)k}$, $\forall k \geq 1$ be an auxiliary sequence with $\hat{\rho}_1 = 3\sqrt{\frac{\rho_1}{\tau_0}}$, and γ_k be an auxiliary sequence with $\gamma_0 = \frac{\sigma_0}{\tau_0}$, and suppose $\gamma_k, \sigma_k, \tau_k, \theta_k, t_k$ satisfy the relation

$$\tau_0^{-1} \geq L_{XY} + L_G^2 \frac{\sigma_0}{\delta}, \text{ where } \delta \in (0, 1], \quad \text{eq:step-size-0} \quad (18)$$

$$\theta_k = \frac{\sigma_{k-1}}{\sigma_k}, \quad \gamma_{k+1} = \gamma_k (1 + \rho_{k+1} \tau_k), \quad \tau_{k+1} = \tau_k \sqrt{\frac{\gamma_k}{\gamma_{k+1}}}, \quad \text{eq:step-size-1} \quad (19)$$

$$t_k = \frac{\sigma_k}{\sigma_0}, \quad \sigma_{k+1} = \gamma_{k+1} \tau_{k+1}. \quad \text{eq:step-size-2} \quad (20)$$

Then the step-size sequences satisfy

$$\gamma_k \geq \frac{\hat{\rho}_k^2 \tau_0^2 \gamma_0}{9} k^2 + \gamma_0, \quad T_k \geq 1 + \frac{\tau_0}{6} \hat{\rho}_k (k+1)k, \quad \hat{\rho}_k \geq \min\{\rho_1, \hat{\rho}_1\}, \quad \text{speed_lower} \quad (21)$$

where $\tilde{\rho}_k = \frac{2}{k(k+1)} \sum_{s=0}^k \hat{\rho}_s s$ for $k \geq 1$.

Moreover, suppose $\bar{\rho} \tau_0 \leq 2$, where $\bar{\rho} = \bar{c} \cdot \bar{\mu}$, then we have

$$\gamma_k \leq \gamma_0 (k+1)^2. \quad \text{eq:gammak_upper} \quad (22)$$

Proof. Note $\tau_{k+1} = \tau_k \sqrt{\frac{\gamma_k}{\gamma_{k+1}}}$ implies that $\tau_k = \tau_0 \sqrt{\frac{\gamma_0}{\gamma_k}}$. Due to $\gamma_{k+1} = \gamma_k (1 + \rho_{k+1} \tau_k)$, we conclude that $\gamma_{k+1} = \gamma_k (1 + \rho_{k+1} \tau_k) = \gamma_k + \rho_{k+1} \tau_0 \sqrt{\gamma_0 \gamma_k}$.

Next, we use induction to show that

$$\gamma_k \geq \frac{\hat{\rho}_k^2 \tau_0^2 \gamma_0}{9} k^2 + \gamma_0. \quad \text{eq:gamma_k_lower_speed} \quad (23)$$

It is easy to see that the result (23) holds for $k = 0$ and $k = 1$ by the definition of $\hat{\rho}_1$. Assume (23) holds for all $k = 0, \dots, K$, then we have

$$\begin{aligned} \gamma_{K+1} &= \gamma_K + \rho_{K+1} \tau_0 \sqrt{\gamma_0 \gamma_K} \\ &\geq \frac{\hat{\rho}_K^2 \tau_0^2 \gamma_0}{9} K^2 + \gamma_0 + \rho_{K+1} \tau_0 \sqrt{\gamma_0 \frac{\hat{\rho}_K^2 \tau_0^2 \gamma_0}{9} K^2} \\ &= \frac{\tau_0^2 \gamma_0}{9} (\hat{\rho}_K^2 K^2 + 3\rho_{K+1} \hat{\rho}_K K) + \gamma_0 \\ &= \frac{\tau_0^2 \gamma_0}{9} (K+1)^2 \hat{\rho}_{K+1}^2 + \gamma_0, \end{aligned} \quad \text{eq:speed_gamma_induction} \quad (24)$$

which completes our induction. It follows from (23) and the relation among $T_k, t_k, \sigma_k, \tau_k$ that

$$\begin{aligned} T_k &= \sum_{s=0}^k t_s \geq 1 + \sum_{s=1}^k \sqrt{\frac{\tau_0}{\sigma_0}} \sqrt{\frac{\hat{\rho}_s^2 \tau_0^2 \gamma_0}{9} s^2 + \gamma_0} \\ &\geq 1 + \sum_{s=1}^k \frac{\hat{\rho}_s \tau_0}{3} s = 1 + \frac{\tau_0}{3} \sum_{s=1}^k \hat{\rho}_s s = 1 + \frac{\tau_0}{6} \tilde{\rho}_k (k+1)k. \end{aligned} \quad \text{eq:Tk_rate} \quad (25)$$

Similarly, we use induction to prove

$$\hat{\rho}_k \geq \min\{\rho_1, \hat{\rho}_1\}, \quad \forall k \geq 1. \quad \text{eq:induction} \quad (26)$$

It is easy to find that $\hat{\rho}_1 \geq \min\{\rho_1, \hat{\rho}_1\}$. We assume that (26) holds for any $k = 1, \dots, K$. Considering $\hat{\rho}_{K+1}$, we have

$$\begin{aligned} \hat{\rho}_{K+1} &= \frac{1}{K+1} \sqrt{\hat{\rho}_K^2 K^2 + 3\rho_{K+1} \hat{\rho}_K K} \\ &\geq \frac{1}{K+1} \sqrt{\hat{\rho}_K^2 K^2 + 3\rho_1 \hat{\rho}_K K} \end{aligned}$$

Case 1: If $\hat{\rho}_K \geq \hat{\rho}_1 \geq \rho_1$, for $K \geq 1$, we obtain

$$\hat{\rho}_{K+1} \geq \frac{1}{K+1} \sqrt{(\rho_1)^2 K^2 + 3(\rho_1)^2 K} \geq \frac{1}{K+1} \sqrt{(\rho_1)^2 K^2 + 2(\rho_1)^2 K + (\rho_1)^2} = \rho_1. \quad \text{lower_bound_seq_01} \quad (27)$$

Case 2: If $\hat{\rho}_K \geq \rho_1 \geq \hat{\rho}_1$, for $K \geq 1$, we have

$$\rho_{K+1} \geq \frac{1}{K+1} \sqrt{(\hat{\rho}_1)^2 K^2 + 3(\hat{\rho}_1)^2 K} \geq \hat{\rho}_1. \quad \text{lower_bound_seq_02} \quad (28)$$

Combining (27) and (28) yields the result (26). In view of (23), (25), and (26), we complete our proof of (21).

Moreover, we use induction to show $\gamma_k \leq \gamma_0(k+1)^2$. It is obvious that the inequality above holds for $k=0$. Assume the inequality holds for all $k=0, \dots, K$, then we have

$$\begin{aligned} \gamma_{K+1} &= \gamma_K + \rho_{K+1} \tau_0 \sqrt{\gamma_0} \sqrt{\gamma_K} \\ &\leq \gamma_0(K+1)^2 + \rho_{K+1} \tau_0 \gamma_0(K+1) \\ &\leq \gamma_0(K^2 + (2 + \bar{\rho} \tau_0)K + \bar{\rho} \tau_0 + 1) \\ &\leq \gamma_0(K^2 + 4K + 4) = \gamma_0(K+2)^2, \end{aligned}$$

where the second inequality is by $\rho_k \leq \bar{\rho}$ for any k , and the last inequality is by $\bar{\rho} \tau_0 \leq 2$. \square

Corollary 1. Suppose $\gamma_k, \sigma_k, \tau_k, \theta_k, t_k$ satisfy the relation (18), (19) and (20). Then, for any $K \geq 1$, we have

$$\begin{aligned} f(\bar{\mathbf{x}}_K) - f(\mathbf{x}^*) &\leq \frac{6}{6 + \tau_0 \bar{\rho}_K (K+1)K}, \\ \|[G(\bar{\mathbf{x}}_K)]_+\| &\leq \frac{6}{c^*(6 + \tau_0 \bar{\rho}_K (K+1)K)}, \quad \text{eq:cor_complexity} \quad (29) \\ \frac{1}{2} \|\mathbf{x}_K - \mathbf{x}^*\|^2 &\leq \frac{3\sigma_0}{\bar{\rho}_K^2 \tau_0^2 K^2 + 9\gamma_0}, \end{aligned}$$

Remark 2. In view of Corollary 1, APDPro obtains the best $\mathcal{O}(\frac{1}{\sqrt{\bar{\rho}_K \varepsilon}})$ iteration complexity, which is substantially better than the $\mathcal{O}(\frac{1}{\varepsilon})$ bounds of APD [11] and the ConEx [6] when the strong convexity parameter is relatively large compared with ε . In addition, we argue that even when $\bar{\rho}_K = \mathcal{O}(\varepsilon)$, APDPro can obtain the matching $\mathcal{O}(\frac{1}{\varepsilon})$ bound of the state-of-the-art algorithms. Specifically, using the definition of γ_k, σ_k , we can easily derive the monotonicity of $\{\sigma_k\}$,

$$\sigma_{k+1} = \gamma_{k+1} \tau_{k+1} = \tau_k \sqrt{\gamma_k \gamma_{k+1}} = \tau_k \gamma_k \sqrt{1 + \rho_{k+1} \tau_k} \geq \gamma_k \tau_k = \sigma_k,$$

which implies $T_k = \sum_{s=0}^{k-1} t_k = \sigma_0^{-1} \sum_{s=0}^{k-1} \sigma_k \geq k$. Using a similar argument to that of Corollary 1, we immediately obtain the bound $f(\bar{\mathbf{x}}_K) - f(\mathbf{x}^*) \leq \mathcal{O}(\frac{1}{K})$ and $\|[G(\bar{\mathbf{x}}_K)]_+\| \leq \mathcal{O}(\frac{1}{K})$.

Remark 3. The algorithm implementation of APDPro requires knowing an upper bound on $\|\mathbf{y}^*\|$. When the bound is unavailable, [11] developed an adaptive APD which still ensures the boundedness of dual sequence via line search. Since our main goal of this paper is to exploit the *lower-bound* rather than the *upper bound* of $\|\mathbf{y}^*\|$, we leave the extension of our technique to such adaptive APD to the future work.

4 APDPro with a Restart Scheme

Note that in the worst case, APDPro exhibits an iteration complexity of $\mathcal{O}(\frac{D_X}{\sqrt{\varepsilon}} + \frac{D_Y}{\sqrt{\varepsilon}})$, which has linear dependence on the diameter. While the $\mathcal{O}(\frac{1}{\sqrt{\varepsilon}})$ is optimal [27], it is possible to improve the complexity with respect to the primal part from $\mathcal{O}(\frac{D_X}{\sqrt{\varepsilon}})$ to $\mathcal{O}(\log(\frac{D_X}{\sqrt{\varepsilon}}))$. To achieve this goal, we propose a restart scheme (rAPDPro) that calls APDPro repeatedly and present the details in Algorithm 2. The total iteration number of APDPro in each epoch is an important parameter of the restart algorithm. Inspired by [17], we set the iteration number as a function of the estimated strong convexity, detailed in the TERMINATEITER procedure. For the convenience in describing a double-loop algorithm, we use superscripts for the number of epochs and the subscripts for the number of sub-iterations in parameters $\mathbf{x}, \mathbf{y}, \tau, \sigma, \gamma$, e.g., \mathbf{x}_1^S meaning the \mathbf{x} output of first iterations at S -th epoch.

In Theorem 2, we show the overall convergence complexity of rAPDPro.

Algorithm 2 Restarted APDPro (rAPDPro)

Require: $\rho_{N-1}^{-1} \geq 0, \bar{\sigma} > 0, \delta \in (0, 1], \mathbf{x}_{N-1}^{-1}, \mathbf{y}_{N-1}^{-1}, S$

```

1: Compute
2: for  $s = 0, 1, \dots, S$  do
3:   Set  $\tau_0^s = \bar{\tau}, \sigma_0^s = \bar{\sigma}, (\mathbf{x}_{-1}^s, \mathbf{y}_{-1}^s) \leftarrow (\mathbf{x}_{N_{s-1}}^{s-1}, \mathbf{y}_{N_{s-1}}^{s-1}), (\mathbf{x}_0^s, \mathbf{y}_0^s) \leftarrow (\mathbf{x}_{N_{s-1}}^{s-1}, \mathbf{y}_{N_{s-1}}^{s-1}), \rho_0^s = \rho_{N_{s-1}}^{s-1}$ 
4:   Set  $\Delta_{XY} = \frac{1}{\tau_0^s} D_X^2 + \frac{1}{2\sigma_0^s} D_Y^2, \sigma_{-1}^s \leftarrow \sigma_0^s, \gamma_0^s \leftarrow \bar{\gamma}, T_0^s = 0, k = 0, \hat{\rho}_0^s = 1, N_s = \infty$ 
5:   while  $k < N_s$  do
6:     Run line 4-11 of APDPro with index set  $(s, k)$ 
7:     Update  $N_s, \hat{\rho}_{k+1}^s \leftarrow \text{TERMINATEITER}(\hat{\rho}_k^s, \rho_{k+1}^s, s, k)$ 
8:      $k \leftarrow k + 1$ 
9: Output:  $\mathbf{x}_{N_s}^S, \mathbf{y}_{N_s}^S$ 
10: procedure TERMINATEITER( $\hat{\rho}_{\text{old}}, \rho, s, k$ )
11:   Compute  $\hat{\rho}_{\text{new}} = \begin{cases} \frac{1}{k+1} \sqrt{\hat{\rho}_{\text{old}}^2 k^2 + 3\rho \hat{\rho}_{\text{old}} k} & k > 1 \\ 3\sqrt{\rho/\tau_0} & k = 1 \end{cases}$ 
12:   Compute  $N = \lceil \max\{\frac{2\sqrt{3}\sigma_0}{\hat{\rho}_{\text{new}} \bar{\tau}^{1.5}}, \frac{\sqrt{6}D_Y}{\hat{\rho}_{\text{new}} \tau_0 D_X} 2^{\frac{s}{2}}\} \rceil$ 
13:   return  $N, \hat{\rho}_{\text{new}}$ 

```

Theorem 2. Let $\{\mathbf{x}_0^s\}_{s \geq 0}$ be the sequence generated by rAPDPro, then we have

$$\|\mathbf{x}_0^s - \mathbf{x}^*\|^2 \leq \Delta_s \equiv D_X^2 \cdot 2^{-s}, \quad \forall s \geq 0. \quad \text{eq:exp decay} \quad (30)$$

As a consequence, rAPDPro will find a solution \mathbf{x}_0^S such that $\|\mathbf{x}_0^S - \mathbf{x}^*\|^2 \leq \varepsilon$ for any $\varepsilon \in (0, D_X^2)$ in at most $S := \lceil \log_2 \frac{D_X^2}{\varepsilon} \rceil$ epochs. Moreover, the overall number of iterations performed by rAPDPro to find such a solution is bounded by

$$T_\varepsilon := \left(\frac{4\sqrt{3}\bar{\sigma}}{\bar{\tau}^{3/2}} + 2 \right) \left[\log_2 \frac{D_X}{\sqrt{\varepsilon}} + 1 \right] + \frac{2(\sqrt{6} + \sqrt{3})}{\bar{\tau}} \frac{D_Y}{\sqrt{\varepsilon}}, \quad \text{T.6} \quad (31)$$

where $\sum_{s=0}^S (\hat{\rho}_{N_s}^s)^{-1} = (\tilde{\rho}_1)^{-1}(S+1)$ and $\sum_{s=0}^S \frac{\sqrt{2}^s}{\hat{\rho}_{N_s}^s} = (\tilde{\rho}_2)^{-1} \sum_{s=0}^S \sqrt{2}^s$.

Proof. First, we show that the choice of $\tau_0^s = \bar{\tau}, \sigma_0^s = \bar{\sigma}, \forall s \geq 0$ satisfy the condition (18) in Corollary 1:

$$\frac{1}{\tau_0^s} \geq \frac{1-\nu_0}{\tau_0^s} = L_{XY} + \frac{L_G^2}{\delta} \sigma_0^s.$$

Next, we show (30) holds by induction. Clearly, (30) holds for $s = 0$. Assume $\|\mathbf{x}_0^s - \mathbf{x}^*\|^2 \leq \Delta_s$ holds for $s = 0, \dots, S-1$. Then by Theorem 1, we have

$$\begin{aligned} \|\mathbf{x}_0^S - \mathbf{x}^*\|^2 &\leq \frac{\sigma_0^S \tau_{N_S}^S}{\sigma_{N_S}^S} \left(\frac{1}{\tau_0^S} \|\mathbf{x}_0^{S-1} - \mathbf{x}^*\|^2 + \frac{1}{\sigma_0^S} \|\mathbf{y}_0^{S-1} - \mathbf{y}^*\|^2 \right) \\ &\leq \frac{\sigma_0^S \tau_{N_S}^S}{\sigma_{N_S}^S} \left(\frac{2}{\tau_0^S} \Delta_S + \frac{1}{\sigma_0^S} D_Y^2 \right). \end{aligned} \quad \text{eq:restart-01} \quad (32)$$

In view of the bound in (21) and the relation between $\tau_{N_s}^s, \sigma_{N_s}^s, T_{N_s}^s$, we can get

$$\frac{\tau_{N_s}^s}{\sigma_{N_s}^s} \leq \frac{3}{(\hat{\rho}_{N_s}^s \tau_0^s N_s)^2}. \quad \text{eq:restart-02} \quad (33)$$

Combining (32) and (33) yields

$$\begin{aligned} \|\mathbf{x}_0^S - \mathbf{x}^*\|^2 &\leq \frac{3\sigma_0^S}{(\hat{\rho}_{N_S}^S \tau_0^S N_S)^2} \left(\frac{2}{\tau_0^S} \Delta_S + \frac{1}{\sigma_0^S} D_Y^2 \right) \\ &\leq \frac{6\sigma_0^S}{(\hat{\rho}_{N_S}^S \tau_0^S N_S)^2 \tau_0^S} \Delta_S + \frac{3D_Y^2}{(\hat{\rho}_0^S \tau_0^S N_S)^2}. \end{aligned}$$

Due to the definition of N_s , i.e., $N_s = \lceil \max\{\frac{2\sqrt{3\bar{\sigma}}}{\hat{\rho}_{N_s}^s \bar{\tau}^{1.5}}, \frac{\sqrt{6}D_Y}{\hat{\rho}_{N_s}^s \tau_0^s D_X} 2^{\frac{s}{2}}\} \rceil$, then we obtain

$$\begin{aligned} \frac{6\sigma_0^S}{(\hat{\rho}_{N_s}^s \tau_0^s N_s)^2 \tau_0^S} &\leq \frac{6\sigma_0^S}{(\hat{\rho}_{N_s}^s \tau_0^s)^2 \tau_0^S} \cdot \frac{(\hat{\rho}_{N_s}^s)^2 \bar{\tau}^3}{12\sigma_0^S} = \frac{1}{2}, \\ \frac{3D_Y^2}{(\hat{\rho}_{N_s}^s \tau_0^s N_s)^2} &\leq \frac{3D_Y^2}{(\hat{\rho}_{N_s}^s \tau_0^s)^2} \cdot \frac{(\hat{\rho}_{N_s}^s \tau_0^s)^2}{6D_Y^2} \Delta_S = \frac{1}{2} \Delta_S, \end{aligned}$$

which implies the desired result (30).

Suppose the algorithm runs for $S = \lceil \log_2 \frac{D_X^2}{\varepsilon} \rceil$ epochs, then $\|\mathbf{x}_0^S - \mathbf{x}^*\|^2 \leq D_X^2 \cdot 2^{-S} \leq \varepsilon$. It follows from that property (21) that the sequence $\hat{\rho}_{N_s}^s$ is lower bounded, and then we denote $\hat{\rho} := \min_s \{\hat{\rho}_{N_s}^s\}$. The total number of iterations required by Algorithm 2 is

$$\begin{aligned} \sum_{s=0}^S N_s &\leq \sum_{s=0}^S \left\{ \frac{2\sqrt{3\bar{\sigma}}}{\hat{\rho}_{N_s}^s \bar{\tau}^{3/2}} + \frac{\sqrt{6}D_Y}{\hat{\rho}_{N_s}^s \tau_0^s D_X} 2^{\frac{s}{2}} + 1 \right\} \\ &\leq \left(\frac{4\sqrt{3\bar{\sigma}}}{\tilde{\rho}_1 \bar{\tau}^{3/2}} + 2 \right) \left[\log_2 \frac{D_X}{\sqrt{\varepsilon}} + 1 \right] + \left(\frac{\sqrt{6}D_Y}{\tilde{\rho}_2 \bar{\tau} D_X} \right) (2 + \sqrt{2}) (\sqrt{2}^S - \frac{\sqrt{2}}{2}) \\ &\leq \left(\frac{4\sqrt{3\bar{\sigma}}}{\tilde{\rho}_1 \bar{\tau}^{3/2}} + 2 \right) \left[\log_2 \frac{D_X}{\sqrt{\varepsilon}} + 1 \right] + \frac{2(\sqrt{6} + \sqrt{3}) D_Y}{\tilde{\rho}_2 \bar{\tau} \sqrt{\varepsilon}}, \end{aligned}$$

where (a) holds by $\sum_{s=0}^S (\hat{\rho}_{N_s}^s)^{-1} = (\tilde{\rho}_1)^{-1}(S+1)$ and $\sum_{s=0}^S \frac{\sqrt{2}^s}{\hat{\rho}_{N_s}^s} = (\tilde{\rho}_2)^{-1} \sum_{s=0}^S \sqrt{2}^s$. \square

Remark 4. The bound T_ε depends on ε , $\tilde{\rho}_1$ and $\tilde{\rho}_2$. If $\tilde{\rho}_1 = O((-\log_2 \sqrt{\varepsilon})^{-1})$ or $\tilde{\rho}_2 = O(\sqrt{\varepsilon})$, then we have $T_\varepsilon = \infty$, which implies that we can not guarantee $\|\mathbf{x}_0^s - \mathbf{x}^*\| \leq \varepsilon$ at finite iterations. $T_\varepsilon = \infty$ implies that there exists an epoch with infinite sub-iterations. Hence, rAPDPro is reduced to APDPro if we only consider that epoch.

Remark 5. Comparison of rAPDPro and APDPro involves a number of factors. In particular, rAPDPro compares favorably against APDPro if $\|\mathbf{x}_0 - \mathbf{x}^*\|$ is sufficiently large, namely, $\|\mathbf{x}_0 - \mathbf{x}^*\| = \tilde{\Omega}(\sqrt{\varepsilon} \log D_X)$. Moreover, it should be noted that the complexity bound (31) can be slightly improved if D_X is replaced by any tighter upper bound of $\|\mathbf{x}_0^s - \mathbf{x}^*\|$. However, it is still unknown whether we can directly replace D_X with $\|\mathbf{x}_0^s - \mathbf{x}^*\|$ in (31).

Dual Convergence For dual variables, we establish asymptotic convergence to the optimal solution, a property that will play an essential role in developing the active-set identification scheme in the later section. For the sake of analysis, it is more convenient to consider the generated solution as a whole sequence using a single subscript index: $\mathbf{x}_1, \mathbf{x}_2, \dots, \mathbf{x}_N; \mathbf{y}_1, \mathbf{y}_2, \dots, \mathbf{y}_N$. Hence, we use the index system j and (s, k) interchangeably. Note that $\{\mathbf{x}_0^s, \mathbf{y}_0^s\}$ and $\{\mathbf{x}_{N_s+1}^s, \mathbf{y}_{N_s+1}^s\}$ correspond to the same pair of points. Let

$$Q_j(\mathbf{x}, \mathbf{y}) = \frac{(\tau_j)^{-1} - \rho_j}{2} \|\mathbf{x} - \mathbf{x}_j\|^2 + \frac{1}{2\sigma_j} \|\mathbf{y} - \mathbf{y}_j\|^2 + \theta_j \langle \mathbf{y}_j - \mathbf{y}, G(\mathbf{x}_j) - G(\mathbf{x}_{j-1}) \rangle + \frac{\theta_j}{2\delta/\sigma_{j-1}} \|G(\mathbf{x}_j) - G(\mathbf{x}_{j-1})\|^2,$$

then we establish an important recursive property about the solution sequence in the following lemma.

Lemma 2. Assume $\bar{\tau}^{-1} > \bar{\rho}$ and choose $\nu_0 > 0$ such that

$$1 > \inf_{j \geq 0} \{\theta_j\} \geq \delta + \nu_0. \tag{34} \quad \text{eq:ini_step_assu}$$

Then there exists an $\nu_1 > 0$ such that for any $j \geq 0$ and any KKT point $(\mathbf{x}^*, \tilde{\mathbf{y}}^*)$:

$$0 \leq t_j Q_j(\mathbf{x}^*, \tilde{\mathbf{y}}^*) - t_{j+1} Q_{j+1}(\mathbf{x}^*, \tilde{\mathbf{y}}^*) - \nu_1 t_j \left[\frac{1}{2\tau_j} \|\mathbf{x}_{j+1} - \mathbf{x}_j\|^2 + \frac{1}{2\sigma_j} \|\mathbf{y}_{j+1} - \mathbf{y}_j\|^2 \right], \text{ and } t_j Q_j(\mathbf{x}^*, \tilde{\mathbf{y}}^*) > 0. \tag{35} \quad \text{eq:lem_asy_res_new}$$

Remark 6. Assumption $(\bar{\tau})^{-1} > \bar{\rho}$ is mild. Since we always choose $\bar{\sigma}$ large enough in rAPDPro, $\bar{\tau}$ can be arbitrarily small. Furthermore, since $\frac{\sigma_k^s}{\sigma_{k-1}^s} = \frac{1}{\theta_k^s} = \sqrt{1 + \rho_k^s \tau_k^s}$, $\{\rho_k^s\}$ is a bounded sequence by dual variable has an upper bound (Proposition 1), $\{\tau_k^s\}$ is monotonically decreasing, then $\inf_{0 \leq k \leq N_s} \theta_k^s \geq (1 + \bar{\rho}\bar{\tau})^{-1/2}$. Hence, inequality (34) is always satisfiable if we choose proper δ, ν_0 such that $(1 + \bar{\rho}\bar{\tau})^{-1/2} \geq \delta + \nu_0$.

Theorem 3. With the same assumptions of Lemma 2, we have $(\mathbf{x}^*, \mathbf{y}^*)$ satisfy KKT condition, where \mathbf{y}^* is any limit point of $\{\mathbf{y}_j\}$ generated by rAPDPro.

5 A Multi-stage Accelerated Primal-Dual Algorithm

In all the proposed algorithms beforehand, we require to solve a complicated dual problem involving a linear cut constraint. A potential issue is that the corresponding sub-problem may not have a closed-form solution. To resolve this issue, we propose a new method to obtain the same $\mathcal{O}(1/\sqrt{\varepsilon})$ complexity without the need of introducing new cut constraint. We present the Multi-Stage Accelerated Primal-Dual Algorithm (msAPD) in Algorithm 3. Motivated by the restart algorithm, our new method is a double-loop procedure for which an accelerated primal-dual algorithm with pending sub-iteration number (APDPI) is running in each stage. While both APDPI and APDPro employ the IMPROVE step to estimate the dual lower bound, APDPI only relies on the lower bound estimation to change the inner-loop iteration number adaptively, but not the step-size selection. As a consequence, APDPI does not explicitly add dual cut constraints to warrant strong convexity of the Lagrangian function.

Algorithm 3 Multi-Stage APD (msAPD)

Require: $\bar{\mathbf{x}}^0 \in \mathcal{X}, \bar{\mathbf{y}}^0 \in \mathcal{Y}, \delta \in (0, 1], \tilde{\sigma}, S$

```

1: Initialize:  $\rho_0^0 = 0$ 
2: for  $s = 0, \dots, S$  do
3:   Compute  $\tau_0^s = (L_{XY} + \frac{L_G^2 \tilde{\sigma}}{\delta} \cdot 2^{\frac{s}{2}})^{-1}, \sigma_0^s = \tilde{\sigma} \cdot 2^{\frac{s}{2}}$ 
4:    $(\bar{\mathbf{x}}^{s+1}, \bar{\mathbf{y}}^{s+1}, \rho_0^{s+1}) \leftarrow \text{APDPI}(\tau_0^s, \sigma_0^s, \bar{\mathbf{x}}^s, \bar{\mathbf{y}}^s, \rho_0^s, s)$ 
5: Output:  $\bar{\mathbf{x}}^{S+1}, \bar{\mathbf{y}}^{S+1}$ 
6: procedure APDPI( $\tau_0^s, \sigma_0^s, \mathbf{x}_0, \mathbf{y}_0, \rho_0^s, s$ )
7:   Initialize:  $(\mathbf{x}_{-1}, \mathbf{y}_{-1}) \leftarrow (\mathbf{x}_0, \mathbf{y}_0), \bar{\mathbf{x}}_0 = \mathbf{x}_0, k = 0, N_s = \infty$ 
8:   while  $k < N_s$  do
9:      $\mathbf{z}_k \leftarrow 2G(\mathbf{x}_k) - G(\mathbf{x}_{k-1})$ 
10:     $\mathbf{y}_{k+1} \leftarrow \text{PROX}_{\mathbf{0}, \mathcal{Y}}(\mathbf{y}_k, -\mathbf{z}_k, \sigma_0^s)$ 
11:     $\mathbf{x}_{k+1} \leftarrow \text{PROX}_{f, \mathcal{X}}(\mathbf{x}_k, \nabla G(\mathbf{x}_k) \mathbf{y}_{k+1}, \tau_0^s)$ 
12:     $\bar{\mathbf{x}}_{k+1} \leftarrow (k\bar{\mathbf{x}}_k + \mathbf{x}_{k+1}) / (k+1),$ 
13:     $\rho_{k+1}^s \leftarrow \text{IMPROVE}(\mathbf{x}_k, \bar{\mathbf{x}}_k, \frac{1}{2} D_X^2, \frac{\Delta_{XY}}{\rho_k^s}, \rho_k^s)$ 
14:    Compute  $N_s = \lceil \max \{ \frac{4}{\rho_{k+1}^s \tau_0^s}, \frac{D_Y^2}{\rho_{k+1}^s \sigma_0^s D_X^2} \cdot 2^{s+1} \} \rceil$ 
15:     $k \leftarrow k + 1$ 
16:   return  $\bar{\mathbf{x}}_{N_s}, \bar{\mathbf{y}}_{N_s}, \rho_k^s$ 

```

We develop the convergence property of the procedure APDPI, which paves the path to proving our main theorem. For the convergence analysis, it suffices to verify that the initial step-size parameter τ_0^s, σ_0^s satisfy assumptions in Theorem 4. For completeness, We leave the proof in Section D.

Theorem 4. *Let the sequence $\{\bar{\mathbf{x}}_k^s, \bar{\mathbf{y}}_k^s\}_{k \geq 0}$ be generated by APDPI, then we have*

$$\mathcal{L}(\bar{\mathbf{x}}_K^s, \mathbf{y}^*) - \mathcal{L}(\mathbf{x}^*, \bar{\mathbf{y}}_K^s) \leq \frac{1}{K} \Delta^s(\mathbf{x}^*, \mathbf{y}^*), \quad \text{eq:thm4} \tag{36}$$

$$\frac{1}{2} \|\bar{\mathbf{x}}_K^s - \mathbf{x}^*\|^2 \leq \frac{1}{(\mathbf{y}^*)^T \boldsymbol{\mu}_K} \Delta^s(\mathbf{x}^*, \mathbf{y}^*), \quad \text{eq:thm2} \tag{37}$$

where $\Delta^s(\mathbf{x}^*, \mathbf{y}^*) \triangleq \frac{1}{2\tau_0^s} \|\mathbf{x}_0^s - \mathbf{x}^*\|^2 + \frac{1}{2\sigma_0^s} \|\mathbf{y}_0^s - \mathbf{y}^*\|^2$.

We show that msAPD obtains an $\mathcal{O}(1/\sqrt{\varepsilon})$ rate of convergence to the optimal solution, which matches the complexity of APDPro.

Theorem 5. *Let $\{\bar{\mathbf{x}}_0^s\}$ be the sequence computed by msAPD. Then, we have*

$$\|\bar{\mathbf{x}}_0^s - \mathbf{x}^*\|^2 \leq \Delta_s \equiv D_X^2 \cdot 2^{-s}, \quad \forall s \geq 0. \quad \text{eq:ratiodecrease1} \tag{38}$$

For any $\varepsilon \in (0, D_X^2)$, msAPD will find a solution $\bar{\mathbf{x}}_0^s \in \mathcal{X}$ such that $\|\bar{\mathbf{x}}_0^s - \mathbf{x}^*\|^2 \leq \varepsilon$ in at most $\lceil \log_2 \frac{D_X^2}{\varepsilon} \rceil$ epochs. Moreover, the overall iteration number performed by msAPD to find such a solution is bounded by

$$T_\varepsilon = \left(\frac{8L_{XY}}{\rho_{N_0}^0} + 2 \right) \lceil \log_2 \frac{D_X}{\sqrt{\varepsilon}} + 1 \rceil + (2 + \sqrt{2}) \left(\frac{\tilde{\sigma} L_G^2}{\delta} + \frac{2D_Y^2}{\rho_{N_0}^0 \tilde{\sigma} D_X^2} \right) \frac{D_X}{\sqrt{\varepsilon}}.$$

Proof. We first show that (38) holds by induction. It is easy to verify that (38) holds for $s = 0$. Assume $\|\bar{\mathbf{x}}_0^s - \mathbf{x}^*\|^2 \leq \Delta_s = D_X^2 \cdot 2^{-s}$ holds for $s = 0, \dots, S-1$. By Theorem 4, we have

$$\begin{aligned} \|\bar{\mathbf{x}}_0^S - \mathbf{x}^*\|^2 &\leq \frac{1}{(\mathbf{y}^*)^T \boldsymbol{\mu}_{N_{S-1}}} \left(\frac{1}{\tau_0^{S-1}} \|\bar{\mathbf{x}}_0^{S-1} - \mathbf{x}^*\|^2 + \frac{1}{\sigma_0^{S-1}} \|\bar{\mathbf{y}}_0^{S-1} - \mathbf{y}^*\|^2 \right) \\ &\leq \frac{1}{(\mathbf{y}^*)^T \boldsymbol{\mu}_{N_{S-1}}} \left(\frac{2}{\tau_0^{S-1}} \Delta_S + \frac{1}{\sigma_0^{S-1}} D_Y^2 \right) \end{aligned}$$

By the definition of N_s , we have $N_{S-1} = \lceil \max \left\{ \frac{4}{\rho_{N_{S-1}}^{S-1} \tau_0^{S-1}}, \frac{2D_Y^2}{\rho_{N_{S-1}}^{S-1} \sigma_0^{S-1} \Delta_S} \right\} \rceil$ and the following inequalities holds:

$$\begin{aligned} 2((\mathbf{y}^*)^T \boldsymbol{\mu}_{N_{S-1}} \tau_0^{S-1})^{-1} &\leq 2(\rho_{N_{S-1}}^{S-1} N_{S-1} \tau_0^{S-1})^{-1} \leq \frac{2}{\rho_{N_{S-1}}^{S-1} \tau_0^{S-1}} \cdot \frac{\rho_{N_{S-1}}^{S-1} \tau_0^{S-1}}{4} = \frac{1}{2}, \\ D_Y^2 ((\mathbf{y}^*)^T \boldsymbol{\mu}_{N_{S-1}} \sigma_0^{S-1})^{-1} &\leq D_Y^2 (\rho_{N_{S-1}}^{S-1} N_{S-1} \sigma_0^{S-1})^{-1} \leq \frac{D_Y^2}{\rho_{N_{S-1}}^{S-1} \sigma_0^{S-1}} \cdot \frac{\rho_{N_{S-1}}^{S-1} \sigma_0^{S-1}}{2D_Y^2} \Delta_S = \frac{1}{2} \Delta_S. \end{aligned}$$

Putting these pieces together, we have $\|\bar{\mathbf{x}}_S - \mathbf{x}^*\|^2 \leq \frac{1}{2} \Delta_S + \frac{1}{2} \Delta_S = \Delta_S$. Suppose the algorithm runs for S epochs to achieve the desired accuracy ε , i.e., $\|\mathbf{x}_0^S - \mathbf{x}^*\|^2 \leq D_X^2 \cdot 2^{-S} \leq \varepsilon$. Then the overall iteration number can be bounded by

$$\begin{aligned} \sum_{s=0}^S N_s &\stackrel{(a)}{\leq} \sum_{s=0}^S \left\{ \frac{4}{\rho_{N_0}^0 \tau_0^{s-1}} + \frac{2D_Y^2}{\rho_{N_0}^0 \sigma_0^{s-1} \Delta_S} + 1 \right\} \\ &\stackrel{(b)}{\leq} \sum_{s=0}^S \left\{ \left(\frac{4L_{XY}}{\rho_{N_0}^0} + 1 \right) + \left(\frac{\tilde{\sigma} L_G^2}{\delta} + \frac{2D_Y^2}{\rho_{N_0}^0 \tilde{\sigma} D_X^2} \right) \sqrt{2}^s \right\} \\ &\leq \left(\frac{4L_{XY}}{\rho_{N_0}^0} + 1 \right) (S+1) + \left(\frac{\tilde{\sigma} L_G^2}{\delta} + \frac{2D_Y^2}{\rho_{N_0}^0 \tilde{\sigma} D_X^2} \right) (2 + \sqrt{2}) (\sqrt{2}^S - \frac{\sqrt{2}}{2}) \\ &\leq \left(\frac{8L_{XY}}{\rho_{N_0}^0} + 2 \right) \lceil \log_2 \frac{D_X}{\sqrt{\varepsilon}} + 1 \rceil + (2 + \sqrt{2}) \left(\frac{\tilde{\sigma} L_G^2}{\delta} + \frac{2D_Y^2}{\rho_{N_0}^0 \tilde{\sigma} D_X^2} \right) \frac{D_X}{\sqrt{\varepsilon}}, \end{aligned}$$

where (a) holds by $\rho_{N_s}^s \geq \rho_{N_0}^0, \forall s \geq 0$, (b) follows from the definition of τ_0^s and σ_0^s . \square

Remark 7. Theorem 5 shows that msAPD obtains a worst-case complexity of $\mathcal{O}(\log(\frac{D_X}{\sqrt{\varepsilon}}) + (D_X + \frac{D_Y^2}{D_X}) \frac{1}{\sqrt{\varepsilon}})$, which, according to Theorem 2, is an upper bound of the complexity of rAPDPro. The complexities of msAPD and rAPDPro match when $D_X = \Omega(1)D_Y$. Otherwise, rAPDPro appears to be much better in terms of dependence on $\frac{D_X}{\sqrt{\varepsilon}}$. On the other hand, msAPD has a more simple proximal subproblem, which does not involve additional cut constraint on the dual update.

6 Active-set Identification in Sparsity-inducing Optimization

In this section, we apply our proposed algorithms to the aforementioned sparse learning problem:

$$\begin{aligned} \min \quad & f(\mathbf{x}) := \sum_{i=1}^B p_i \|\mathbf{x}_{(i)}\| \\ \text{s.t.} \quad & \mathbf{x} = \mathbf{x}_{(1)} \times \dots \times \mathbf{x}_{(B)}, \mathbf{x}_{(i)} \in \mathbb{R}^{n_i}, 1 \leq i \leq B \\ & g(\mathbf{x}) \leq 0, \end{aligned} \tag{39}$$

where $f(\mathbf{x})$ is the group Lasso regularizer and $g(\mathbf{x})$ is a strongly convex function. We use subscripts $\mathbf{x}_{(i)}$ to express the i -th block coordinates of \mathbf{x} . For notation convenience, we write $f_i(\mathbf{x}_{(i)}) = p_i \|\mathbf{x}_{(i)}\|$. A notable example is the Lasso problem where $B = n, p_i = 1, \forall i$, and $\mathbf{x}_{(i)}$ is a real value and we write $f(\mathbf{x}) = \sum_i |\mathbf{x}_{(i)}|$. As has been shown in the earlier sections, our proposed algorithms APDPro, rAPDPro and msAPD exhibit an $\mathcal{O}(\frac{1}{\sqrt{\varepsilon}})$ rate of convergence. The goal of this section is to show that rAPDPro can identify sparsity pattern

of the optimal solution of (39) in finite number of iterations. Identification property of other algorithms can be established analogously.

In general, suppose that a function $f(\mathbf{x})$ has a separable structure $f(\mathbf{x}) = \sum_{i=1}^B f_i(\mathbf{x}_{(i)})$, we define the active set $\mathcal{A}(\mathbf{x})$ for $f(\mathbf{x})$ by

$$\mathcal{A}(\mathbf{x}) := \{i : \partial f_i(\mathbf{x}_{(i)}) \text{ is not a singleton}\}.$$

For the objective in (39), it is easy to see that $\mathcal{A}(\mathbf{x}^*)$ is the index set of the zero blocks: $\mathcal{A}(\mathbf{x}^*) = \{i : \mathbf{x}_{(i)}^* = \mathbf{0}\}$. Next, we describe some properties for the optimal solution of (39).

Proposition 5. *Under Assumption 1 and 2, the optimal solution \mathbf{x}^* and Lagrangian multiplier \mathbf{y}^* satisfying the KKT condition for problem (39) is unique.*

Proof. The uniqueness of primal optimal solution \mathbf{x}^* follows from Proposition 2. The KKT condition (ensured by Slater's CQ) implies

$$\mathbf{0} \in \partial f(\mathbf{x}^*) + \nabla g(\mathbf{x}^*)\mathbf{y}^*. \tag{40} \text{eq:kkt-3}$$

According to Assumption 2, we have $\mathbf{x}^* \neq \mathbf{0}$, hence $\mathcal{A}^c(\mathbf{x}^*) = \{1, 2, \dots, B\} \setminus \mathcal{A}(\mathbf{x}^*) \neq \emptyset$. In view of (40), for any $i \in \mathcal{A}^c(\mathbf{x}^*)$, we have $p_i \frac{\mathbf{x}_{(i)}^*}{\|\mathbf{x}_{(i)}^*\|} = -\nabla_{(i)}g(\mathbf{x}^*)\mathbf{y}^*$, which gives a unique \mathbf{y}^* . \square

In order to identify sparsity pattern (active set) of the optimal solution, it is common to assume the existence of a non-degenerate optimal solution, which is stronger than the standard optimality condition (see [26, 29]). We say that \mathbf{x}^* is non-degenerate if $\mathbf{0} \in \text{ri} \partial \mathcal{L}(\mathbf{x}^*, \mathbf{y}^*) = \text{ri}(\partial f(\mathbf{x}^*) + \nabla g(\mathbf{x}^*)\mathbf{y}^*)$ for the Lagrangian multiplier \mathbf{y}^* , where ri stands for the relative interior. More specifically, $(\mathbf{x}^*, \mathbf{y}^*)$ satisfies the block-wise optimality condition

$$\begin{cases} -[\nabla g(\mathbf{x}^*)\mathbf{y}^*]_{(i)} = \nabla f_i(\mathbf{x}_{(i)}^*), & \text{if } i \notin \mathcal{A}(\mathbf{x}^*), \\ -[\nabla g(\mathbf{x}^*)\mathbf{y}^*]_{(i)} \in \text{int}(\partial f_i(\mathbf{x}_{(i)}^*)), & \text{if } i \in \mathcal{A}(\mathbf{x}^*). \end{cases}$$

Inspired by [26], we consider the following definition of η , which describes the certain distance between gradient and "subdifferential boundary" of active set.

$$\eta := \min_{i \in \mathcal{A}(\mathbf{x}^*)} \{p_i - \|[\nabla g(\mathbf{x}^*)\mathbf{y}^*]_{(i)}\|\}.$$

Our proof strategy of active-set identification in rAPDPro is similar to the identification result in unconstrained optimization [26]. Namely, we show that optimal sparsity pattern is identified when the iterates fall in a properly defined neighborhood dependent on η . The next lemma shows that the primal and dual sequence indeed converge to the neighbourhood of the optimal primal and dual solutions, respectively, in a finite number of iterations.

Lemma 3. *There exists an \hat{S}_1 such that*

$$\|\mathbf{x}_0^s - \mathbf{x}^*\| \leq \|\mathbf{x}_0^{\hat{S}_1} - \mathbf{x}^*\| \quad \text{and} \quad \|\mathbf{y}_0^s - \mathbf{y}^*\| \leq \|\mathbf{y}_0^{\hat{S}_1} - \mathbf{y}^*\|, \forall s \geq \hat{S}_1, \tag{41} \text{eq:def_hat_s1}$$

where $(\mathbf{x}^*, \mathbf{y}^*)$ is the unique solution of problem (39). Moreover, there exists an epoch $\hat{S}_0 \geq \hat{S}_1$ such that

$$\|\mathbf{y}_k^s - \mathbf{y}^*\| \leq \frac{\eta}{3\|\nabla g(\mathbf{x}^*)\|}, \quad \|\mathbf{x}_k^s - \mathbf{x}^*\| \leq \frac{\eta}{3L_{XY}} \frac{\tau_k^s}{\tau_k^s + (2L_{XY})^{-1}}, \quad \forall s \geq \hat{S}_0, \quad \forall k = 0, 1, \dots, N_s. \tag{42} \text{x_small-1}$$

It is worth noting that the primal neighbourhood defined by the second term of (42) is bit different from the fixed neighborhood in the standard analysis [26] which involves a constant stepsize. As APDPro sets $\tau_k^s = \mathcal{O}(\frac{1}{k})$, both the point distance and neighborhood radius decay at the same $\mathcal{O}(\frac{1}{k})$ rate. Hence, we use a substantially different analysis to show the sparsity identification in the constrained setting.

Theorem 6. *In rAPDPro, suppose we choose $\zeta > \frac{\eta}{3L_{XY}} \frac{\bar{\tau}}{\bar{\tau} + (2L_{XY})^{-1}}$ in defining \mathcal{X} , then we have*

$$\mathbf{x}_{(i)}^* = \mathbf{x}_{k(i)}^s, s \geq \hat{S}_0, \quad \forall k \in [N_s], \quad \forall i \in \mathcal{A}(\mathbf{x}^*).$$

Proof. It follows from Lipschitz smoothness of $g(\cdot)$ and property (42) that for any $s \geq \hat{S}_0$, we have

$$\begin{aligned} & \left\| [\nabla g(\mathbf{x}_k^s) \mathbf{y}_{k+1}^s]_{(i)} \right\| - \left\| [\nabla g(\mathbf{x}^*) \mathbf{y}_{k+1}^s]_{(i)} \right\| \\ & \leq \left\| \nabla g(\mathbf{x}_k^s) \mathbf{y}_{k+1}^s - \nabla g(\mathbf{x}^*) \mathbf{y}_{k+1}^s \right\| \\ & \leq L_{XY} \left\| \mathbf{x}_k^s - \mathbf{x}^* \right\| \leq \frac{\eta}{3} \frac{\tau_k^s}{\tau_k^s + (2L_{XY})^{-1}}, \quad k = 0, \dots, N_s. \end{aligned} \tag{43}$$

Recall that the primal update has the following form

$$\mathbf{x}_{k+1}^s = \operatorname{argmin}_{\mathbf{x} \in \mathcal{X}} \left\{ \sum_{i=1}^B p_i \|\mathbf{x}_{(i)}\| + \langle \nabla g(\mathbf{x}_k^s) \mathbf{y}_{k+1}^s, \mathbf{x} \rangle + \frac{1}{2\tau_k^s} \|\mathbf{x} - \mathbf{x}_k^s\|^2 \right\}.$$

Since $\frac{\tau_k^s}{\tau_k^s + (2L_{XY})^{-1}}$ is monotonically increasing with respect to τ_k^s , we have

$$\|\mathbf{x}_{k+1}^s - \tilde{\mathbf{x}}\| \leq \|\mathbf{x}_{k+1}^s - \mathbf{x}^*\| + \|\mathbf{x}^* - \tilde{\mathbf{x}}\| \stackrel{(a)}{\leq} \frac{\eta}{3L_{XY}} \frac{\tau_k^s}{\tau_k^s + (2L_{XY})^{-1}} + \|\mathbf{x}^* - \tilde{\mathbf{x}}\| \stackrel{(b)}{<} \zeta + \min_{i \in [m]} 2\sqrt{\frac{-2g_i(\mathbf{x}_i^*)}{\mu_i}}, \tag{44}$$

where . Inequality (44) implies that $\mathbf{x}_{k+1}^s \in \mathbf{int} \mathcal{X}$, and hence $\mathcal{N}_{\mathcal{X}}(\mathbf{x}_{k+1}^s) = \{\mathbf{0}\}$. In view of the optimality condition, we have

$$\left[\frac{1}{\tau_k^s} (\mathbf{x}_k^s - \mathbf{x}_{k+1}^s) - \nabla g(\mathbf{x}_k^s) \mathbf{y}_{k+1}^s \right]_{(i)} \in p_i \partial \|\mathbf{x}_{k+1}^s\|_{(i)}, \quad 1 \leq i \leq B. \tag{45}$$

Our next goal is to show $[\mathbf{x}_{k+1}^s]_{(i)} = \mathbf{x}_{(i)}^*$ satisfies condition (45) for $i \in \mathcal{A}(\mathbf{x}^*)$. Placing $\mathbf{x}_{(i)} = \mathbf{x}_{(i)}^*$ in $\left\| \left[\nabla g(\mathbf{x}_k^s) \mathbf{y}_{k+1}^s + \frac{1}{\tau_k^s} (\mathbf{x} - \mathbf{x}_k^s) \right]_{(i)} \right\|$, we have

$$\begin{aligned} & \left\| \left[\nabla g(\mathbf{x}_k^s) \mathbf{y}_{k+1}^s + \frac{1}{\tau_k^s} (\mathbf{x}^* - \mathbf{x}_k^s) \right]_{(i)} \right\| \\ & \leq \left\| \left[\nabla g(\mathbf{x}_k^s) \mathbf{y}_{k+1}^s \right]_{(i)} \right\| + \left\| \frac{1}{\tau_k^s} (\mathbf{x}_{(i)}^* - \mathbf{x}_{k(i)}^s) \right\| \\ & \stackrel{(a)}{\leq} \frac{\eta}{3} \frac{\tau_k^s}{\tau_k^s + (2L_{XY})^{-1}} + \left\| \left[\nabla g(\mathbf{x}^*) \mathbf{y}_{k+1}^s \right]_{(i)} \right\| + \frac{\eta}{3} \frac{(L_{XY})^{-1}}{\tau_k^s + (2L_{XY})^{-1}} \\ & \stackrel{(b)}{\leq} \frac{\eta}{3} \left[\frac{\tau_k^s + 2(2L_{XY})^{-1}}{\tau_k^s + (2L_{XY})^{-1}} + 1 \right] + \left\| \left[\nabla g(\mathbf{x}^*) \mathbf{y}^* \right]_{(i)} \right\| \\ & < \eta + \left\| \left[\nabla g(\mathbf{x}^*) \mathbf{y}^* \right]_{(i)} \right\| \\ & \stackrel{(c)}{\leq} p_i, \quad \forall i \in \mathcal{A}(\mathbf{x}^*). \end{aligned} \tag{46}$$

In above, (a) follows from (42) and (43), (b) follows from $\left\| \left[\nabla g(\mathbf{x}^*) \mathbf{y}_{k+1}^s \right]_{(i)} \right\| - \left\| \left[\nabla g(\mathbf{x}^*) \mathbf{y}^* \right]_{(i)} \right\| \leq \|\mathbf{y}_{k+1}^s - \mathbf{y}^*\| \|\nabla g(\mathbf{x}^*)\| \leq \frac{\eta}{3}$, and (c) holds by the definition of η . Combining (45) and (46), we have $\mathcal{A}(\mathbf{x}^*) \subseteq \mathcal{A}(\mathbf{x}_{k+1}^s)$, $s \geq \hat{S}_0$, $\forall k \in [N_s]$, which complete our proof. \square

7 Numerical study

In this section, we examine the empirical performance of our proposed algorithms for solving the lasso type problem (2). We implement both rAPDPro and msAPD. We skip APDPro as we observe that restart strategy consistently improves the algorithm performance. For comparison, we consider Mirror-Prox [13] and the state-of-the-art accelerated primal-dual (APD) method [11]. All experiments are performed on a machine running 64-bit Windows 10 with Intel i7-10710U @ 1.10GHz and 16GB DDR4.

Experiment setup In (2) the only constraint is $g(\mathbf{x}) = \frac{1}{2} \|\mathbf{A}\mathbf{x} - \mathbf{b}\|^2 - u$, where u is the target loss level, and we assume A has full column rank. In the simulation, we generate matrix A with its elements from Gaussian distribution. The recovered sparse solution \mathbf{x} has 10% nonzero elements, which are also generated from the Gaussian distribution. Then we set $\mathbf{b} = \mathbf{A}\mathbf{x} + \varepsilon$, where ε is generated by Gaussian distribution,

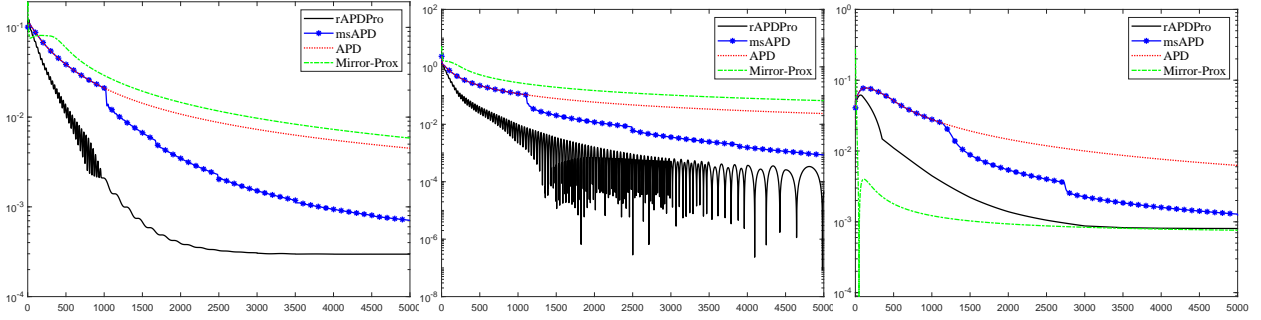


Figure 1: x -axis: iteration number. y -axis: $\log_{10}((\|\mathbf{x}_k\|_1 - \|\mathbf{x}^*\|_1)/\|\mathbf{x}^*\|_1)$ for rAPDPro, $\log_{10}((\|\bar{\mathbf{x}}_k\|_1 - \|\mathbf{x}^*\|_1)/\|\mathbf{x}^*\|_1)$ for APD, msAPD and Mirror-Prox (\mathbf{x}^* is computed by IPM implemented in Mosek).

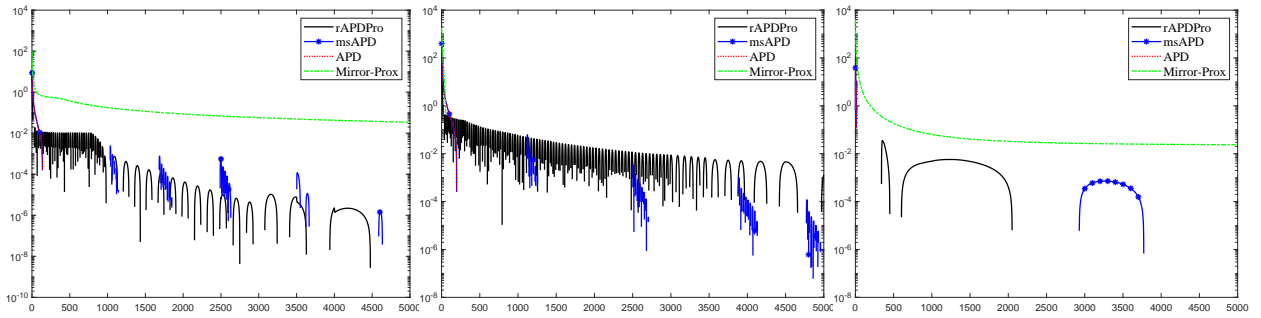


Figure 2: x -axis: Iteration number. y -axis: feasibility gap is $\log_{10}(\max\{0, G(\mathbf{x}_k)\})$ for rAPDPro, $\log_{10}(\max\{0, G(\bar{\mathbf{x}}_k)\})$ for APD, msAPD and Mirror-Prox.

too. Finally, choose proper u such that $\{\mathbf{x} \mid \frac{1}{2}\|\mathbf{A}\mathbf{x} - \mathbf{b}\|^2 \leq u\}$ is nonempty. We randomly generated three datasets for which A is of size 128×32 , 256×128 and 500×300 , and \mathbf{b} , u accordingly. We set $r = 1$ in (7) and $\underline{\mu} = \lambda_{\min}(A^T A)$, where $\lambda_{\min}(\cdot)$ computes the minimal eigenvalue. The Lipschitz constants defined in (10) and (8) can be set as $L_X \triangleq \lambda_{\max}(A^T A)$, $L_{XY} \triangleq \frac{-\|\tilde{\mathbf{x}}\|_1}{\frac{1}{2}\|\mathbf{A}\tilde{\mathbf{x}} - \mathbf{b}\|^2 - u} \cdot \lambda_{\max}(A^T A)$, where $\tilde{\mathbf{x}}$ is the solution of $\min_{\mathbf{x}} \|\mathbf{A}\mathbf{x} - \mathbf{b}\|^2$. Other parameters (i.e. \mathcal{X} , D_X , D_Y) can be computed accordingly.

Parameter tuning In APDPro, the estimated strong convexity modulus can be sometimes too conservative. Intuitively, as the algorithm converges, we have $\mathbf{x}_k, \mathbf{x}_{k-1} \rightarrow \mathbf{x}^*$. Hence, it is reasonable to use $\|\nabla g(\mathbf{x}_k) - \nabla g(\mathbf{x}_{k-1})\| \leq L_X^{\text{local}} \|\mathbf{x}_k - \mathbf{x}_{k-1}\|$ to provide a gradually refined estimation of the Lipschitz constant L_X in IMPROVE. In msAPD, we apply a similar strategy to estimate L_G and L_{XY} locally, i.e., via $|g(\mathbf{x}_k) - g(\mathbf{x}_{k-1})| \leq L_G^{\text{local}} \|\mathbf{x}_k - \mathbf{x}_{k-1}\|$ and $L_{XY}^{\text{local}} \triangleq \frac{f(\tilde{\mathbf{x}})}{-g(\tilde{\mathbf{x}})} L_X^{\text{local}}$. Moreover, to prevent the algorithm from staying in a single epoch for too long (due to conservative parameter estimation), we switch the epoch whenever pre-specified maximum iteration number is reached. Finally, we adopt the above empirical strategies throughout our experiments; a separate comparative study shows that these strategies can substantially improve the performance of our proposed algorithms.

We compare the convergence performance of the proposed algorithms. We plot the relative function value gap $|f(\mathbf{x}) - f(\mathbf{x}^*)|/|f(\mathbf{x}^*)|$ and the feasibility violation $\max\{g(\mathbf{x}), 0\}$ over the iteration number in Figure 1 and Figure 2, respectively. First, we observe that APD is able to generate feasible solutions in all the datasets, however, it appears to have an inferior performance in reducing the objective value. In contrast, Mirror-Prox often exhibits a large infeasibility error. Second, it is interesting to compare the performance of msAPD and APD. Notice that both msAPD and APD employ the same step-size rules while msAPD can further leverage the strong convexity to improve the convergence rate. Our results confirm the empirical advantage of the multi-stage strategy. Third, we notice that rAPDPro outperforms the other algorithms in all the datasets.

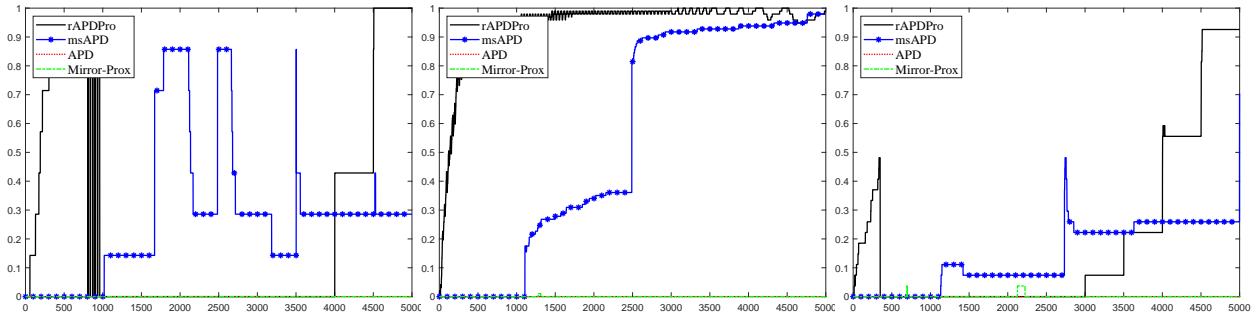


Figure 3: x -axis: iteration number. y -axis: accuracy in active-set identification.

The experimental results seem to confirm the theoretical advantage of the restart strategy in rAPDPro.

Next, we examine the effectiveness of identifying sparsity patterns. We computed a nearly optimal solution \mathbf{x}^* from interior point method. Note that \mathbf{x}^* is a dense vector. For numerical consideration, we truncate the coordinate values of \mathbf{x}^* to zero if the absolute value is below 10^{-6} and perform the same truncation to all the generated solutions of the compared algorithms. Then we use formula $|\mathcal{A}(\mathbf{x}) \cap \mathcal{A}(\mathbf{x}^*)|/|\mathcal{A}(\mathbf{x}^*)|$ to measure the accuracy of identifying the active set, where $|\cdot|$ denotes the cardinality of set. For rAPDPro we consider the last iterate \mathbf{x}_k while for APD, msAPD and Mirror-Prox we plot the result on $\bar{\mathbf{x}}_k$, as these are the solutions where the convergence rates are established. Figure 3 plots the experiment result, from which we observe that rAPDPro is the most efficient algorithm in identifying the active set. While msAPD can also exploit the active set, it will escape from the active set solutions from time to time. This is also consistent with our theoretical analysis. On the other hand, APD and Mirror-Prox appears to perform the worst in identifying the sparsity pattern as they use simple uniform averaging to obtain the solution. Hence, the experimental result show a great potential of our proposed algorithms in identifying sparsity structure in the constrained setting.

8 Conclusion

The key contribution of this paper is that we develop several new first-order primal-dual algorithm for convex optimization with strongly convex constraints. Using some novel strategies to exploit the strong convexity of Lagrangian function, we substantially improves the best convergence rate from $\mathcal{O}(1/\varepsilon)$ to $\mathcal{O}(1/\sqrt{\varepsilon})$. In the application of constrained sparse learning problem, experimental study confirms the advantage of our propose algorithms against state-of-the-art first order methods for constrained optimization. Moreover, we show that one of our proposed algorithms rAPDPro has the favorable feature of identifying the sparsity pattern in the optimal solution. For future work, one direction is to apply adaptive strategy, such as line search, to our framework for dealing with the case when dual bound is unavailable. It also would be interesting to consider more general convex objective when the prox operator is not easy to compute. Another interesting direction is to further exploit the active set identification property in a general setting. For example, it would be interesting to incorporate our algorithm with active constraint identification, which could be highly desirable when there are a large number of constraints.

References

- [1] A. Y. ARAVKIN, J. V. BURKE, D. DRUSVYATSKIY, M. P. FRIEDLANDER, AND S. ROY, *Level-set methods for convex optimization*, Mathematical Programming, 174 (2019), pp. 359–390.
- [2] A. BAYANDINA, P. DVURECHENSKY, A. GASNIKOV, F. STONYAKIN, AND A. TITOV, *Mirror descent and convex optimization problems with non-smooth inequality constraints*, in Large-scale and distributed optimization, Springer, 2018, pp. 181–213.

- [3] A. BECK, *First-order methods in optimization*, SIAM, 2017.
- [4] D. P. BERTSEKAS, *Nonlinear programming*, Athena Scientific, 1999.
- [5] D. BOOB, Q. DENG, AND G. LAN, *Level constrained first order methods for function constrained optimization*, arXiv preprint arXiv:2205.08011, (2022).
- [6] ———, *Stochastic first-order methods for convex and nonconvex functional constrained optimization*, Mathematical Programming, (2022), pp. 1–65.
- [7] G. BRAUN, A. CARDERERA, C. W. COMBETTES, H. HASSANI, A. KARBASI, A. MOKHTARI, AND S. POKUTTA, *Conditional gradient methods*, arXiv preprint arXiv:2211.14103, (2022).
- [8] A. CHAMBOLLE AND T. POCK, *On the ergodic convergence rates of a first-order primal–dual algorithm*, Mathematical Programming, 159 (2016), pp. 253–287.
- [9] J. C. DUNN, *Rates of convergence for conditional gradient algorithms near singular and nonsingular extremals*, SIAM Journal on Control and Optimization, 17 (1979), pp. 187–211.
- [10] D. GARBER AND E. HAZAN, *Faster rates for the frank-wolfe method over strongly-convex sets*, in International Conference on Machine Learning, PMLR, 2015, pp. 541–549.
- [11] E. Y. HAMEDANI AND N. S. AYBAT, *A primal-dual algorithm with line search for general convex-concave saddle point problems*, SIAM Journal on Optimization, 31 (2021), pp. 1299–1329.
- [12] W. L. HARE AND A. S. LEWIS, *Identifying active constraints via partial smoothness and prox-regularity*, Journal of Convex Analysis, 11 (2004), pp. 251–266.
- [13] N. HE, A. JUDITSKY, AND A. NEMIROVSKI, *Mirror prox algorithm for multi-term composite minimization and semi-separable problems*, Computational Optimization and Applications, 61 (2015), pp. 275–319.
- [14] F. IUTZELER AND J. MALICK, *Nonsmoothness in machine learning: specific structure, proximal identification, and applications*, Set-Valued and Variational Analysis, 28 (2020), pp. 661–678.
- [15] M. JOURNÉE, Y. NESTEROV, P. RICHTÁRIK, AND R. SEPULCHRE, *Generalized power method for sparse principal component analysis.*, Journal of Machine Learning Research, 11 (2010).
- [16] A. JUDITSKY, A. NEMIROVSKI, ET AL., *First order methods for nonsmooth convex large-scale optimization, ii: utilizing problems structure*, Optimization for Machine Learning, 30 (2011), pp. 149–183.
- [17] G. LAN, *First-order and stochastic optimization methods for machine learning*, Springer, 2020.
- [18] G. LAN AND R. D. MONTEIRO, *Iteration-complexity of first-order penalty methods for convex programming*, Mathematical Programming, 138 (2013), pp. 115–139.
- [19] ———, *Iteration-complexity of first-order augmented lagrangian methods for convex programming*, Mathematical Programming, 155 (2016), pp. 511–547.
- [20] G. LAN AND Z. ZHOU, *Algorithms for stochastic optimization with expectation constraints*, arXiv preprint arXiv:1604.03887, (2016).
- [21] S. LEE, S. J. WRIGHT, AND L. BOTTOU, *Manifold identification in dual averaging for regularized stochastic online learning.*, Journal of Machine Learning Research, 13 (2012).
- [22] E. S. LEVITIN AND B. T. POLYAK, *Constrained minimization methods*, USSR Computational mathematics and mathematical physics, 6 (1966), pp. 1–50.
- [23] Q. LIN, S. NADARAJAH, AND N. SOHEILI, *A level-set method for convex optimization with a feasible solution path*, SIAM Journal on Optimization, 28 (2018), pp. 3290–3311.

- [24] T. LIN, C. JIN, AND M. I. JORDAN, *Near-optimal algorithms for minimax optimization*, in Conference on Learning Theory, PMLR, 2020, pp. 2738–2779.
- [25] Y. NESTEROV, *Dual extrapolation and its applications to solving variational inequalities and related problems*, Mathematical Programming, 109 (2007), pp. 319–344.
- [26] J. NUTINI, M. SCHMIDT, AND W. HARE, “*active-set complexity*” of proximal gradient: *How long does it take to find the sparsity pattern?*, Optimization Letters, 13 (2019), pp. 645–655.
- [27] Y. OUYANG AND Y. XU, *Lower complexity bounds of first-order methods for convex-concave bilinear saddle-point problems*, Mathematical Programming, 185 (2021), pp. 1–35.
- [28] H. ROBBINS AND D. SIEGMUND, *A convergence theorem for non negative almost supermartingales and some applications*, in Optimizing methods in statistics, Elsevier, 1971, pp. 233–257.
- [29] Y. SUN, H. JEONG, J. NUTINI, AND M. SCHMIDT, *Are we there yet? manifold identification of gradient-related proximal methods*, in The 22nd International Conference on Artificial Intelligence and Statistics, PMLR, 2019, pp. 1110–1119.
- [30] R. TIBSHIRANI, *Regression shrinkage and selection via the lasso*, Journal of the Royal Statistical Society: Series B (Methodological), 58 (1996), pp. 267–288.
- [31] P. TSENG, *On accelerated proximal gradient methods for convex-concave optimization*, submitted to SIAM Journal on Optimization, 2 (2008).
- [32] S. J. WRIGHT, *Identifiable surfaces in constrained optimization*, SIAM Journal on Control and Optimization, 31 (1993), pp. 1063–1079.
- [33] Y. XU, *First-order methods for constrained convex programming based on linearized augmented lagrangian function*, Informs Journal on Optimization, 3 (2021), pp. 89–117.
- [34] ———, *Iteration complexity of inexact augmented lagrangian methods for constrained convex programming*, Mathematical Programming, 185 (2021), pp. 199–244.
- [35] T. YANG, Q. LIN, AND L. ZHANG, *A richer theory of convex constrained optimization with reduced projections and improved rates*, in International Conference on Machine Learning, PMLR, 2017, pp. 3901–3910.

A Auxiliary Lemmas

Lemma 4 (Property 1 in [31]). Let $f : \mathbb{R}^n \rightarrow \mathbb{R} \cup \{+\infty\}$ be a closed strongly convex function with modulus $\mu \geq 0$. Give $\bar{\mathbf{x}} \in \mathcal{X}$, where \mathcal{X} is a compact convex set and $t \geq 0$, let

$$\mathbf{x}^+ = \operatorname{argmin}_{\mathbf{x} \in \mathcal{X}} f(\mathbf{x}) + \frac{t}{2} \|\mathbf{x} - \bar{\mathbf{x}}\|^2,$$

then for all $\mathbf{x} \in \mathcal{X}$, the following inequality holds

$$f(\mathbf{x}) + \frac{t}{2} \|\mathbf{x} - \bar{\mathbf{x}}\|^2 \geq f(\mathbf{x}^+) + \frac{t}{2} \|\mathbf{x}^+ - \mathbf{x}\|^2 + \frac{t}{2} \|\mathbf{x}^+ - \bar{\mathbf{x}}\|^2 + \frac{\mu}{2} \|\mathbf{x} - \mathbf{x}^+\|^2.$$

Lemma 5. Let $\{a_j\}, \{b_j\}$ and $\{c_j\}$ be non-negative real sequences such that $a_{j+1} \leq a_j - b_j + c_j$ for all $j \geq 0$, and $\sum_{j=0}^{\infty} c_j < \infty$. Then $a = \lim_{j \rightarrow \infty} a_j$ exists, and $\sum_{j=0}^{\infty} b_j < \infty$.

Proof. Complete proof can be found in [28]. □

B Proof Details in Section 3

The main proof of Theorem 1 is based on the modification of [11].

B.1 Proof of Theorem 1

Proof. First, it is easy to verify by our construction that $\{\mathcal{Y}_k\}$ is a monotone sequence: $\mathcal{Y}_1 \supseteq \mathcal{Y}_2 \supseteq \dots \supseteq \mathcal{Y}_k \dots$. Our goal is to show $\mathcal{Y}^* \subseteq \mathcal{Y}_k$ holds for any $k \geq 0$ by induction. Note that $\mathcal{Y}^* \subseteq \mathcal{Y}_0$ immediately follows from our assumption that $(\mathbf{y}^*)^T \boldsymbol{\mu} \geq \rho_0$, for any $\mathbf{y}^* \in \mathcal{Y}^*$. Suppose that $\mathcal{Y}^* \subseteq \mathcal{Y}_k$ holds for $k = 0, \dots, K-1$, we claim:

1. For any $\mathbf{x} \in \mathcal{X}$ and $\mathbf{y} \in \mathcal{Y}^*$, we have

$$\mathcal{L}(\bar{\mathbf{x}}_K, \mathbf{y}) - \mathcal{L}(\mathbf{x}, \bar{\mathbf{y}}_K) \leq \frac{1}{T_K} \Delta(\mathbf{x}, \mathbf{y}) - \frac{t_{K-1} \tau_{K-1}^{-1}}{2T_K} \|\mathbf{x} - \mathbf{x}_K\|^2. \quad \text{eq:thm2} \tag{47}$$

2. $\mathcal{Y}^* \subseteq \mathcal{Y}_K$.

Part 1. For $k = 0, 1, 2, \dots, K-1$, taking $-\langle \mathbf{z}_k, \cdot \rangle$ and $f(\cdot) + \langle \nabla G(\mathbf{x}_k) \mathbf{y}_{k+1}, \cdot \rangle$ in Lemma 4, the following relations

$$-\langle \mathbf{y}_{k+1} - \mathbf{y}, \mathbf{z}_k \rangle \leq A_{k+1}, \quad \text{eq:indicator} \tag{48}$$

$$f(\mathbf{x}_{k+1}) + \langle \mathbf{y}_{k+1}, \nabla G(\mathbf{x}_k)^T (\mathbf{x}_{k+1} - \mathbf{x}) \rangle \leq f(\mathbf{x}) + B_{k+1}, \quad \text{eq:inequality} \tag{49}$$

where

$$A_{k+1} \triangleq \frac{1}{2\sigma_k} (\|\mathbf{y} - \mathbf{y}_k\|^2 - \|\mathbf{y} - \mathbf{y}_{k+1}\|^2 - \|\mathbf{y}_{k+1} - \mathbf{y}_k\|^2),$$

$$B_{k+1} \triangleq \frac{1}{2\tau_k} (\|\mathbf{x} - \mathbf{x}_k\|^2 - \|\mathbf{x} - \mathbf{x}_{k+1}\|^2 - \|\mathbf{x}_{k+1} - \mathbf{x}_k\|^2),$$

hold for any $\mathbf{x} \in \mathcal{X}$ and $\mathbf{y} \in \bigcap_{0 \leq s \leq k} \mathcal{Y}_s$. The existence of such \mathbf{y} follows from our induction hypothesis.

Since $\mathbf{y}_{k+1}^T G(\cdot)$ is ρ_k -strongly convex, we have

$$\begin{aligned} & \langle \mathbf{y}_{k+1}, \nabla G(\mathbf{x}_k)^T (\mathbf{x}_{k+1} - \mathbf{x}) \rangle \\ &= \langle \mathbf{y}_{k+1}, \nabla G(\mathbf{x}_k)^T (\mathbf{x}_{k+1} - \mathbf{x}_k) \rangle + \langle \mathbf{y}_{k+1}, \nabla G(\mathbf{x}_k)^T (\mathbf{x}_k - \mathbf{x}) \rangle \\ &\geq \langle \mathbf{y}_{k+1}, \nabla G(\mathbf{x}_k)^T (\mathbf{x}_{k+1} - \mathbf{x}_k) \rangle + \langle \mathbf{y}_{k+1}, G(\mathbf{x}_{k+1}) - G(\mathbf{x}) \rangle - \langle \mathbf{y}_{k+1}, G(\mathbf{x}_{k+1}) - G(\mathbf{x}_k) \rangle + \frac{\rho_k}{2} \|\mathbf{x} - \mathbf{x}_k\|^2. \end{aligned}$$

Combining this result and (49), we have

$$\begin{aligned} & f(\mathbf{x}_{k+1}) - f(\mathbf{x}) + \langle \mathbf{y}_{k+1}, G(\mathbf{x}_{k+1}) - G(\mathbf{x}) \rangle \\ &\leq B_{k+1} - \langle \mathbf{y}_{k+1}, \nabla G(\mathbf{x}_k)^T (\mathbf{x}_{k+1} - \mathbf{x}_k) \rangle + \langle \mathbf{y}_{k+1}, G(\mathbf{x}_{k+1}) - G(\mathbf{x}_k) \rangle - \frac{\rho_k}{2} \|\mathbf{x} - \mathbf{x}_k\|^2. \end{aligned} \quad \text{eq:temp-01} \tag{50}$$

On the other hand, by the definition of \mathbf{z}_k , we have

$$\begin{aligned}
& \langle \mathbf{y} - \mathbf{y}_{k+1}, \mathbf{z}_k \rangle \\
&= \langle \mathbf{y} - \mathbf{y}_{k+1}, G(\mathbf{x}_k) \rangle + \theta_k \langle \mathbf{y} - \mathbf{y}_{k+1}, G(\mathbf{x}_k) - G(\mathbf{x}_{k-1}) \rangle \\
&= \langle \mathbf{y} - \mathbf{y}_{k+1}, G(\mathbf{x}_k) - G(\mathbf{x}_{k+1}) \rangle + \langle \mathbf{y} - \mathbf{y}_{k+1}, G(\mathbf{x}_{k+1}) \rangle \\
&\quad + \theta_k \langle \mathbf{y} - \mathbf{y}_k, G(\mathbf{x}_k) - G(\mathbf{x}_{k-1}) \rangle + \theta_k \langle \mathbf{y}_k - \mathbf{y}_{k+1}, G(\mathbf{x}_k) - G(\mathbf{x}_{k-1}) \rangle.
\end{aligned} \tag{51}$$

Let us denote $\mathbf{q}_k = G(\mathbf{x}_k) - G(\mathbf{x}_{k-1})$ for brevity. Combining (48) and (51) yields

$$\langle \mathbf{y} - \mathbf{y}_{k+1}, G(\mathbf{x}_{k+1}) \rangle \leq A_{k+1} + \langle \mathbf{y} - \mathbf{y}_{k+1}, G(\mathbf{x}_{k+1}) - G(\mathbf{x}_k) \rangle - \theta_k \langle \mathbf{y} - \mathbf{y}_k, \mathbf{q}_k \rangle - \theta_k \langle \mathbf{y}_k - \mathbf{y}_{k+1}, \mathbf{q}_k \rangle. \tag{52}$$

Putting (50) and (52) together, we have

$$\begin{aligned}
& \mathcal{L}(\mathbf{x}_{k+1}, \mathbf{y}) - \mathcal{L}(\mathbf{x}, \mathbf{y}_{k+1}) \\
&= f(\mathbf{x}_{k+1}) - f(\mathbf{x}) + \langle \mathbf{y}, G(\mathbf{x}_{k+1}) \rangle - \langle \mathbf{y}_{k+1}, G(\mathbf{x}) \rangle \\
&\leq A_{k+1} + B_{k+1} - \langle \mathbf{y}_{k+1}, \nabla G(\mathbf{x}_k)^T (\mathbf{x}_{k+1} - \mathbf{x}_k) \rangle + \langle \mathbf{y}_{k+1}, G(\mathbf{x}_{k+1}) - G(\mathbf{x}_k) \rangle \\
&\quad + \langle \mathbf{y} - \mathbf{y}_{k+1}, \mathbf{q}_{k+1} \rangle - \theta_k \langle \mathbf{y} - \mathbf{y}_k, \mathbf{q}_k \rangle + \theta_k \langle \mathbf{y}_{k+1} - \mathbf{y}_k, \mathbf{q}_k \rangle - \frac{\rho_k}{2} \|\mathbf{x} - \mathbf{x}_k\|^2 \\
&\leq A_{k+1} + B_{k+1} + \frac{L_{XY}}{2} \|\mathbf{x}_{k+1} - \mathbf{x}_k\|^2 - \frac{\rho_k}{2} \|\mathbf{x} - \mathbf{x}_k\|^2 \\
&\quad + \langle \mathbf{y} - \mathbf{y}_{k+1}, \mathbf{q}_{k+1} \rangle - \theta_k \langle \mathbf{y} - \mathbf{y}_k, \mathbf{q}_k \rangle + \theta_k \langle \mathbf{y}_{k+1} - \mathbf{y}_k, \mathbf{q}_k \rangle,
\end{aligned}$$

where the last inequality is by Lipschitz of $\langle \mathbf{y}_{k+1}, G(\cdot) \rangle$.

Next, we bound the term $\langle \mathbf{q}_k, \mathbf{y}_{k+1} - \mathbf{y}_k \rangle$ by Young's inequality, which gives

$$\langle \mathbf{y}_{k+1} - \mathbf{y}_k, \mathbf{q}_k \rangle \leq \frac{\delta/\sigma_{k-1}}{2} \|\mathbf{y}_{k+1} - \mathbf{y}_k\|^2 + \frac{1}{2\delta/\sigma_{k-1}} \|\mathbf{q}_k\|^2 \tag{53}$$

where δ is a positive constant. It follows from (53) and $\frac{1}{2\delta/\sigma_k} \|\mathbf{q}_{k+1}\|^2 \leq \frac{L_G^2}{2\delta/\sigma_k} \|\mathbf{x}_{k+1} - \mathbf{x}_k\|^2$ that

$$\begin{aligned}
& \mathcal{L}(\mathbf{x}_{k+1}, \mathbf{y}) - \mathcal{L}(\mathbf{x}, \mathbf{y}_{k+1}) \\
&\leq \frac{\tau_k^{-1} - \rho_k}{2} \|\mathbf{x} - \mathbf{x}_k\|^2 - \frac{\tau_k^{-1}}{2} \|\mathbf{x} - \mathbf{x}_{k+1}\|^2 + \frac{\theta_k}{2\delta/\sigma_{k-1}} \|\mathbf{q}_k\|^2 - \frac{1}{2\delta/\sigma_k} \|\mathbf{q}_{k+1}\|^2 \\
&\quad + \frac{1}{2\sigma_k} (\|\mathbf{y} - \mathbf{y}_k\|^2 - \|\mathbf{y} - \mathbf{y}_{k+1}\|^2) + \langle \mathbf{y} - \mathbf{y}_{k+1}, \mathbf{q}_{k+1} \rangle - \theta_k \langle \mathbf{y} - \mathbf{y}_k, \mathbf{q}_k \rangle \\
&\quad - \frac{\sigma_k^{-1} - \theta_k \delta/\sigma_{k-1}}{2} \|\mathbf{y}_{k+1} - \mathbf{y}_k\|^2 + \frac{L_G^2}{2\delta/\sigma_k} \|\mathbf{x}_{k+1} - \mathbf{x}_k\|^2 - \frac{\tau_k^{-1} - L_{XY}}{2} \|\mathbf{x}_{k+1} - \mathbf{x}_k\|^2.
\end{aligned} \tag{54}$$

Multiply both sides of the above relation by t_k and sum up the result for $k = 0, 1, \dots, K-1$. In view of the parameter relation (15) and (16), we have

$$\begin{aligned}
& \sum_{k=0}^{K-1} t_k [\mathcal{L}(\mathbf{x}_{k+1}, \mathbf{y}) - \mathcal{L}(\mathbf{x}, \mathbf{y}_{k+1})] \\
&\leq \frac{t_0(\tau_0^{-1} - \rho_0)}{2} \|\mathbf{x} - \mathbf{x}_0\|^2 - \frac{t_{K-1}\tau_{K-1}^{-1}}{2} \|\mathbf{x} - \mathbf{x}_K\|^2 + \frac{t_0\theta_0}{2\alpha_0} \|\mathbf{q}_0\|^2 - \frac{t_{K-1}}{2\delta/\sigma_{k-1}} \|\mathbf{q}_K\|^2 \\
&\quad + \frac{t_0\sigma_0^{-1}}{2} \|\mathbf{y} - \mathbf{y}_0\|^2 - \frac{t_{K-1}\sigma_{K-1}^{-1}}{2} \|\mathbf{y} - \mathbf{y}_K\|^2 + t_{K-1} \langle \mathbf{y} - \mathbf{y}_K, \mathbf{q}_K \rangle - t_0\theta_0 \langle \mathbf{y} - \mathbf{y}_0, \mathbf{q}_0 \rangle \\
&\stackrel{(a)}{\leq} \frac{t_0(\tau_0^{-1} - \rho_0)}{2} \|\mathbf{x} - \mathbf{x}_0\|^2 - \frac{t_{K-1}\tau_{K-1}^{-1}}{2} \|\mathbf{x} - \mathbf{x}_K\|^2 - \frac{t_{K-1}}{2\delta/\sigma_{k-1}} \|\mathbf{q}_K\|^2 \\
&\quad + \frac{t_0\sigma_0^{-1}}{2} \|\mathbf{y} - \mathbf{y}_0\|^2 - \frac{t_{K-1}\sigma_{K-1}^{-1}}{2} \|\mathbf{y} - \mathbf{y}_K\|^2 + t_{K-1} \langle \mathbf{y} - \mathbf{y}_K, \mathbf{q}_K \rangle - t_0\theta_0 \langle \mathbf{y} - \mathbf{y}_0, \mathbf{q}_0 \rangle \\
&\stackrel{(b)}{\leq} \frac{1}{2\tau_0} \|\mathbf{x} - \mathbf{x}_0\|^2 + \frac{1}{2\sigma_0} \|\mathbf{y} - \mathbf{y}_0\|^2 - \frac{t_{K-1}\tau_{K-1}^{-1}}{2} \|\mathbf{x} - \mathbf{x}_K\|^2 - \frac{(1-\delta)t_{K-1}\sigma_{K-1}^{-1}}{2} \|\mathbf{y} - \mathbf{y}_K\|^2
\end{aligned} \tag{55}$$

where (a) uses $\mathbf{q}_0 = \mathbf{0}$, $\mathbf{x}_{-1} = \mathbf{x}_0$, and (b) holds by $t_0 = 1$, $t_{K-1} \langle \mathbf{y} - \mathbf{y}_K, \mathbf{q}_K \rangle \leq \frac{t_{K-1}\delta/\sigma_{K-1}}{2} \|\mathbf{y} - \mathbf{y}_K\|^2 + \frac{t_{K-1}}{2\delta/\sigma_{K-1}} \|\mathbf{q}_K\|^2$. Moreover, recall that $\bar{\mathbf{x}}_k = T_k^{-1} \sum_{s=0}^{k-1} t_s \mathbf{x}_{s+1}$ and $\bar{\mathbf{y}}_k = T_k^{-1} \sum_{s=0}^{k-1} t_s \mathbf{y}_s$. Since $\mathcal{L}(\mathbf{x}, \mathbf{y})$ is

convex in \mathbf{x} and linear in \mathbf{y} , we have

$$T_K[\mathcal{L}(\bar{\mathbf{x}}_K, \mathbf{y}) - \mathcal{L}(\mathbf{x}, \bar{\mathbf{y}}_K)] \leq \sum_{k=0}^{K-1} t_k [\mathcal{L}(\mathbf{x}_{k+1}, \mathbf{y}) - \mathcal{L}(\mathbf{x}, \mathbf{y}_{k+1})]. \quad \text{eq:temp-05} \quad (56)$$

Combining (55) and (56), we obtain

$$T_K[\mathcal{L}(\bar{\mathbf{x}}_K, \mathbf{y}) - \mathcal{L}(\mathbf{x}, \bar{\mathbf{y}}_K)] \leq \frac{1}{2\tau_0} \|\mathbf{x} - \mathbf{x}_0\|^2 + \frac{1}{2\sigma_0} \|\mathbf{y} - \mathbf{y}_0\|^2 - \frac{t_{K-1}\tau_{K-1}^{-1}}{2} \|\mathbf{x} - \mathbf{x}_K\|^2 - \frac{(1-\delta)t_{K-1}\sigma_{K-1}^{-1}}{2} \|\mathbf{y} - \mathbf{y}_K\|^2. \quad \text{eq:mid-03} \quad (57)$$

Dividing both sides by T_K , we obtain the desired result (47).

Part 2. Next we show $\mathcal{Y}^* \subseteq \mathcal{Y}_K$. Let \mathbf{y}^* be any point in \mathcal{Y}^* . Since (57) holds for any $\mathbf{x} \in \mathcal{X}$ and $\mathbf{y} \in \cap_{0 \leq k \leq K-1} \mathcal{Y}_k \supseteq \mathcal{Y}^*$, we can place $\mathbf{x} = \mathbf{x}^*, \mathbf{y} = \mathbf{y}^* \in \mathcal{Y}^*$ in (47) to obtain

$$\frac{t_{K-1}\tau_{K-1}^{-1}}{2T_K} \|\mathbf{x}^* - \mathbf{x}_K\|^2 + \mathcal{L}(\bar{\mathbf{x}}_K, \mathbf{y}^*) - \mathcal{L}(\mathbf{x}^*, \bar{\mathbf{y}}_K) \leq \frac{1}{T_K} \Delta(\mathbf{x}^*, \mathbf{y}^*).$$

Moreover, the strong convexity of $\mathcal{L}(\cdot, \mathbf{y}^*)$ implies

$$\mathcal{L}(\bar{\mathbf{x}}_K, \mathbf{y}^*) \geq \mathcal{L}(\mathbf{x}^*, \mathbf{y}^*) + \frac{(\mathbf{y}^*)^T \boldsymbol{\mu}}{2} \|\bar{\mathbf{x}}_K - \mathbf{x}^*\|^2 \geq \mathcal{L}(\mathbf{x}^*, \bar{\mathbf{y}}_K) + \frac{(\mathbf{y}^*)^T \boldsymbol{\mu}}{2} \|\bar{\mathbf{x}}_K - \mathbf{x}^*\|^2.$$

Applying the above two inequalities gives

$$\frac{(\mathbf{y}^*)^T \boldsymbol{\mu}}{2} \|\bar{\mathbf{x}}_K - \mathbf{x}^*\|^2 \leq \frac{1}{T_K} \Delta(\mathbf{x}^*, \mathbf{y}^*), \quad \frac{1}{2} \|\mathbf{x}_K - \mathbf{x}^*\|^2 \leq \frac{\tau_{K-1}\sigma_0}{\sigma_{K-1}} \Delta(\mathbf{x}^*, \mathbf{y}^*). \quad \text{eq:thm2-temp04} \quad (58)$$

In view of (58) and proposition 4, we have that

$$(\mathbf{y}^*)^T \boldsymbol{\mu} \geq \underline{\mu} \|\mathbf{y}^*\|_1 = \underline{\mu} \max\{h_1(\mathbf{x}_K, \frac{\sigma_0\tau_{K-1}\Delta_{XY}}{\sigma_{K-1}}), h_2(\bar{\mathbf{x}}_K, \frac{\Delta_{XY}}{T_K})\} := \hat{\rho}_K.$$

Moreover, since $\mathcal{Y}^* \subseteq \mathcal{Y}_{K-1}$, we have $(\mathbf{y}^*)^T \boldsymbol{\mu} \geq \rho_{K-1}$. Hence we have $(\mathbf{y}^*)^T \boldsymbol{\mu} \geq \rho_K$ where $\rho_K = \max\{\hat{\rho}_K, \rho_{K-1}\}$ is the output of the IMPROVE procedure. Due to the construction of \mathcal{Y}_K , we immediately see that $\mathbf{y}^* \in \mathcal{Y}_K$. This implies $\mathcal{Y}^* \subseteq \mathcal{Y}_K$ and completes our induction proof. \square

B.2 Proof of Corollary 1

Proof. First, we show that the sequences $\{\tau_k, \sigma_k, t_k, \theta_k, \rho_k\}_{k \geq 0}$ generated by APDPro satisfy the relationship in (15) and (16) in Theorem 1. The first part of (15) can be derived using the monotonicity of $\{\rho_k\}$ and $\{\gamma_k\}$ as follows:

$$\begin{aligned} t_{k+1}(\tau_{k+1}^{-1} - \rho_{k+1}) &= \sigma_0^{-1} \sigma_{k+1} (\tau_{k+1}^{-1} - \rho_{k+1}) \\ &= \sigma_0^{-1} (\gamma_{k+1} - \gamma_{k+1} \rho_{k+1} \tau_{k+1}) \\ &= \sigma_0^{-1} (\gamma_k + \gamma_k \rho_{k+1} \tau_k - \sqrt{\gamma_{k+1} \gamma_k} \rho_{k+1} \tau_k) \\ &\leq \sigma_0^{-1} \gamma_k = t_k \tau_k^{-1}. \end{aligned}$$

The rest of (15) can be easily verified using the parameters setting (19).

Next, we prove the first term in (16) by induction. Firstly, it is easy to verify that for any $\sigma_0 > 0$, there exists $\tau_0 \in (0, (L_{XY} + L_G^2 \sigma_0 / \delta)^{-1}]$ such that (18) holds. Hence, when $k = 0$, the first term in (16) is directly from (18). Suppose that the first inequality in (16) holds for $k = 0, \dots, K-1$. From $\theta_K = \frac{\sigma_{K-1}}{\sigma_K} = \frac{\tau_K}{\tau_{K-1}} \leq 1$, we have

$$\frac{1}{\tau_K} = \frac{1}{\tau_{K-1} \theta_K} \geq \frac{L_{XY}}{\theta_K} + \frac{L_G^2 \sigma_{K-1} \delta^{-1}}{\theta_K} \geq L_{XY} + L_G^2 \sigma_K \delta^{-1}. \quad \text{eq:relation_tau} \quad (59)$$

Without loss of generality, place $\mathbf{x} = \mathbf{x}^*, \mathbf{y} = \mathbf{y}^+ := (\|\mathbf{y}^*\|_1 + c^*) \frac{[G(\bar{\mathbf{x}}_K)]_+}{\|[G(\bar{\mathbf{x}}_K)]_+\|}$ in (47), and using (6) in Proposition 1. It is easy to see $\|\mathbf{y}^+\| = \|\mathbf{y}^*\|_1 + c^* \leq \bar{c}$, and $\|\mathbf{y}^+\|_1 \geq \|\mathbf{y}^*\|_1 + c^* \geq \|\mathbf{y}^*\|_1$. Hence, we conclude that $\mathbf{y}^+ \in \mathcal{Y}_k, \forall k \geq 0$.

Now observe that $\mathcal{L}(\bar{\mathbf{x}}_K, \mathbf{y}^*) - \mathcal{L}(\mathbf{x}^*, \mathbf{y}^*) \geq 0$, which implies that

$$f(\bar{\mathbf{x}}_K) + \langle \mathbf{y}^*, G(\bar{\mathbf{x}}_K) \rangle - f(\mathbf{x}^*) \geq 0.$$

In view of $\langle \mathbf{y}^*, G(\bar{\mathbf{x}}_K) \rangle \leq \langle \mathbf{y}^*, [G(\bar{\mathbf{x}}_K)]_+ \rangle \leq \|\mathbf{y}^*\| \cdot \|[G(\bar{\mathbf{x}}_K)]_+\|$, then we have

$$f(\bar{\mathbf{x}}_K) + \|\mathbf{y}^*\| \cdot \|[G(\bar{\mathbf{x}}_K)]_+\| - f(\mathbf{x}^*) \geq 0. \quad \text{eq:info1} \quad (60)$$

Moreover, we have

$$\begin{aligned} \mathcal{L}(\bar{\mathbf{x}}_K, \mathbf{y}^+) - \mathcal{L}(\mathbf{x}^*, \bar{\mathbf{y}}_K) &\geq \mathcal{L}(\bar{\mathbf{x}}_K, \mathbf{y}^+) - \mathcal{L}(\mathbf{x}^*, \mathbf{y}^*) \\ &= f(\bar{\mathbf{x}}_K) + (\|\mathbf{y}^*\|_1 + c^*) \|[G(\bar{\mathbf{x}}_K)]_+\| - f(\mathbf{x}^*) \\ &\geq f(\bar{\mathbf{x}}_K) + (\|\mathbf{y}^*\| + c^*) \|[G(\bar{\mathbf{x}}_K)]_+\| - f(\mathbf{x}^*). \end{aligned} \quad \text{eq:info2} \quad (61)$$

Combining (60), (61) and (47), we obtain

$$\max \{c^* \|[G(\bar{\mathbf{x}}_K)]_+\|, f(\bar{\mathbf{x}}_K) - f(\mathbf{x}^*)\} \leq \frac{1}{T_K} \Delta(\mathbf{x}^*, \mathbf{y}^+) \leq, \quad \text{eq:bound-01} \quad (62)$$

In view of the bound in (21) and the relation between τ_k, σ_k, T_k , we can get

$$\frac{\tau_k}{\sigma_k} \leq \frac{3}{\bar{\rho}_k^2 \tau_0^2 k^2 + 9\gamma_0}. \quad \text{speed:extend} \quad (63)$$

In view of (62) and (21), we have

$$\max \{c^* \|[G(\bar{\mathbf{x}}_K)]_+\|, f(\bar{\mathbf{x}}_K) - f(\mathbf{x}^*)\} \leq \frac{6}{6 + \tau_0 \bar{\rho}_K (K+1)K}.$$

Combining (47) and (63) yields

$$\frac{1}{2} \|\mathbf{x}_K - \mathbf{x}^*\|^2 \leq \frac{3\sigma_0}{\bar{\rho}_K^2 \tau_0^2 K^2 + 9\gamma_0}.$$

□

C Proof Details in Section 4

C.1 Proof of Lemma 2

Proof. First, we give some results that will be used in following repeatedly. In view of Lemma 1, and the parameter ergodic sequence generated by rAPDPro, we have $\{(\tau_k^s)^{-1}, \sigma_k^s\}$ is monotonically increasing sequence in k , $\bar{\tau} = \tau_0^s, \bar{\sigma} = \sigma_0^s, \theta_0^s = 1, t_0^s = 1, \forall s \geq 0$, and there exist an $\nu_3 > 0$ such that $\bar{\sigma} + \nu_3 \leq \underline{\sigma} := \min_s \{\sigma_{N_s}^s\}$. Now, for rAPDPro, we claim that

1. For any $j \geq 0$, we have

$$\min \{(\sigma_j^{-1} - \theta_j \delta / \sigma_{j-1}) \sigma_j, (\tau_j^{-1} - L_{XY} - L_G^2 \sigma_j / \delta) \tau_j\} \geq \nu_1, \quad \text{eq:nu-1_ineq} \quad (64)$$

and

$$t_j \min \left\{ \frac{1}{\tau_j} - \rho_j, \frac{1}{\sigma_j} - \frac{\delta}{\sigma_{j-1}} \right\} \geq \nu_2. \quad \text{eq:nu-2_ineq} \quad (65)$$

2. For any $j \geq 0$, we have

$$0 \leq t_j Q_j(\mathbf{x}^*, \tilde{\mathbf{y}}^*) - t_{j+1} Q_{j+1}(\mathbf{x}^*, \tilde{\mathbf{y}}^*) - \nu_1 t_j \left(\frac{1}{2\tau_j} \|\mathbf{x}_{j+1} - \mathbf{x}_j\|^2 + \frac{1}{2\sigma_j} \|\mathbf{y}_{j+1} - \mathbf{y}_j\|^2 \right). \quad \text{eq:res_lem} \quad (66)$$

Part 1. We first consider two subsequent points \mathbf{x}_j and \mathbf{x}_{j+1} within the same epoch, and assume $j \sim (s, k)$. Then, it follows from $\theta_k^s = \frac{\sigma_{k-1}^s}{\sigma_k^s}$ that

$$(\sigma_k^s)^{-1} - \theta_k^s \delta (\sigma_{k-1}^s)^{-1} = (\sigma_k^s)^{-1} - \delta (\sigma_k^s)^{-1} = \frac{1-\delta}{\sigma_k^s} \stackrel{(34)}{\geq} \frac{\nu_0}{\sigma_k^s}. \quad \text{mid_o-01} \quad (67)$$

Next, we use induction to show

$$\frac{1-\nu_0}{\tau_k^s} \geq L_{XY} + L_G^2 \sigma_k^s \delta^{-1}. \quad \text{eq:new_relationship (68)}$$

When $k = 0$, inequality (68) degenerates as the . Suppose (68) holds for $k = 0, 1, \dots, K-1$. Then, from $\theta_K^s = \frac{\sigma_{K-1}^s}{\sigma_K^s} = \frac{\tau_K^s}{\tau_{K-1}^s} \leq 1$, we have

$$(1-\nu_0)(\tau_K^s)^{-1} = (1-\nu_0)(\tau_{K-1}^s \theta_K^s)^{-1} \geq \frac{L_{XY}}{\theta_K^s} + \frac{L_G^2 \sigma_{K-1}^s \delta^{-1}}{\theta_K^s} \geq L_{XY} + L_G^2 \sigma_K^s \delta^{-1},$$

which completes our induction proof. Hence, combining (67) and (68), we have

$$(\sigma_k^s - \theta_k^s \delta / \sigma_{k-1}^s) \sigma_k^s \geq \nu_0, \quad \forall k \in [N_s]. \quad \text{eq:step_size_mid01 (69)}$$

Furthermore, when switching to the next epoch ($s \rightarrow s+1$), we have

$$\begin{aligned} \sigma_0^{s+1} ((\sigma_0^{s+1})^{-1} - \theta_0^{s+1} \delta / \sigma_{N_s}^s) &\stackrel{(a)}{\geq} \sigma_0^{s+1} ((\sigma_0^{s+1})^{-1} - (\sigma_{N_s}^s)^{-1}) \stackrel{(b)}{\geq} 1 - \sigma_0^{s+1} \underline{\sigma}^{-1} \\ &\stackrel{(c)}{\geq} ((\tau_0^{s+1})^{-1} - L_{XY} - L_G^2 \delta^{-1} \sigma_0^{s+1}) \tau_0^{s+1} \geq \nu_0 \tau_0^{s+1} = \nu_0 \bar{\tau}, \end{aligned} \quad \text{eq:step_size_mid02 (70)}$$

where (a) holds by $\theta_0^s = 1$, $\delta < 1$, (b) follows from $(\sigma_{N_s}^s)^{-1} \geq \underline{\sigma}^{-1}$. Hence, combining (67), (69) and (70), we completes our proof of (64) by setting $\nu_1 = \min\{1 - \bar{\sigma} \underline{\sigma}^{-1}, \nu_0 \bar{\tau}, \nu_0\}$.

Since rAPDPro reset the step-size periodically and $\{t_k^s, (\tau_k^s)^{-1}\}_{k \in [N_s]}$ are two monotonically increasing sequences, hence

$$\inf_{j \geq 0} t_j (\frac{1}{\tau_j} - \rho_j) \geq t_0^s (\frac{1}{\bar{\tau}} - \bar{\rho}) = \bar{\tau}^{-1} - \bar{\rho}. \quad \text{eq:step_size_03 (71)}$$

Consider $\inf_{k \in [N_s]} t_k^s \sigma_k^s (1 - \delta \frac{\sigma_k^s}{\sigma_{k-1}^s})$. Combining $\delta + \nu_0 \leq \inf_{k \in [N_s]} \{\theta_k^s\}$, then

$$\inf_{k \in [N_s]} t_k^s \sigma_k (1 - \delta \frac{\sigma_k^s}{\sigma_{k-1}^s}) = \inf_{k \in [N_s]} t_k^s \sigma_k^s (1 - \delta / \theta_k^s) \geq \nu_0 \bar{\sigma}. \quad \text{mid05 (72)}$$

Furthermore, when switching to the next epoch ($s \rightarrow s+1$), we have

$$\inf_{s \geq 0} t_0^{s+1} ((\tau_0^{s+1})^{-1} - \rho_0^{s+1}) \geq (\bar{\tau})^{-1} \inf_{s \geq 0} t_0^{s+1} (\frac{1}{\sigma_0^{s+1}} - \frac{\delta}{\sigma_{N_s}^s}) \stackrel{(a)}{\geq} \inf_{s \geq 0} t_0^{s+1} (\frac{1-\delta}{\underline{\sigma}}) = \frac{1-\delta}{\underline{\sigma}}, \quad \text{eq:step_size_04 (73)}$$

where (a) holds by $(\sigma_0^{s+1})^{-1} \geq (\underline{\sigma})^{-1} \geq (\sigma_{N_s}^s)^{-1}$. Hence, it follows from (71), (72) and (73) that there exist $\nu_2 = \min\{\frac{1}{\bar{\tau}} - \bar{\rho}, \nu_0 \bar{\sigma}, \frac{1-\delta}{\underline{\sigma}}\}$ such (65) holds.

Part 2. for any $j \geq 0$,

$$\begin{aligned} &t_j (\frac{(\tau_j)^{-1}}{2} \|\mathbf{x}^* - \mathbf{x}_{j+1}\|^2 + \frac{1}{2\sigma_j} \|\tilde{\mathbf{y}}^* - \mathbf{y}_{j+1}\|^2 \\ &\quad + \langle G(\mathbf{x}_{j+1}) - G(\mathbf{x}_j), \mathbf{y}_{j+1} - \tilde{\mathbf{y}}^* \rangle + \frac{1}{2\delta/\sigma_j} \|G(\mathbf{x}_{j+1}) - G(\mathbf{x}_j)\|^2) \\ &\geq t_{j+1} Q_{j+1}(\mathbf{x}^*, \tilde{\mathbf{y}}^*). \end{aligned} \quad \text{eq:mid_res_lem03 (74)}$$

Consider $k \in \{0, 1, \dots, N_s\}$. Inequality (34) implies (15) and (16) hold, i.e., $t_{k+1}^s ((\tau_{k+1}^s)^{-1} - \rho_{k+1}^s) \leq t_k^s (\tau_k^s)^{-1}$, $t_{k+1}^s (\sigma_{k+1}^s)^{-1} \leq t_k^s (\sigma_k^s)^{-1}$, $t_{k+1}^s \theta_{k+1}^s = t_k^s \theta_k^s \delta / \sigma_{k-1}^s \leq (\sigma_k^s)^{-1}$ (see proof of Corollary 1 in Section B.2 for more details). Hence, for we have

$$\begin{aligned} &t_k^s (\frac{(\tau_k^s)^{-1}}{2} \|\mathbf{x}^* - \mathbf{x}_{k+1}^s\|^2 + \frac{1}{2\sigma_k^s} \|\tilde{\mathbf{y}}^* - \mathbf{y}_{k+1}^s\|^2 \\ &\quad + \langle G(\mathbf{x}_{k+1}^s) - G(\mathbf{x}_k^s), \mathbf{y}_{k+1}^s - \tilde{\mathbf{y}}^* \rangle + \frac{1}{2\delta/\sigma_k^s} \|G(\mathbf{x}_{k+1}^s) - G(\mathbf{x}_k^s)\|^2) \\ &\geq t_{k+1}^s \left[\frac{(\tau_{k+1}^s)^{-1} - \rho_{k+1}^s}{2} \|\mathbf{x}^* - \mathbf{x}_{k+1}^s\|^2 + \frac{1}{2\sigma_{k+1}^s} \|\tilde{\mathbf{y}}^* - \mathbf{y}_{k+1}^s\|^2 \right. \\ &\quad \left. + \theta_{k+1}^s \langle \mathbf{y}_{k+1}^s - \tilde{\mathbf{y}}^*, G(\mathbf{x}_{k+1}^s) - G(\mathbf{x}_k^s) \rangle + \frac{\theta_{k+1}^s}{2\delta/\sigma_k^s} \|G(\mathbf{x}_{k+1}^s) - G(\mathbf{x}_k^s)\|^2 \right] \\ &= t_{j+1} Q_{j+1}(\mathbf{x}^*, \tilde{\mathbf{y}}^*), \end{aligned} \quad \text{eq:mid_res_lem01 (75)}$$

where j corresponds to (s, k) . Furthermore, consider switching to next epoch ($s \rightarrow s+1$).

$$t_{N_s}^s (\tau_{N_s}^s)^{-1} \geq t_0^{s+1} (\tau_0^{s+1})^{-1} - \rho_0^{s+1} t_0^{s+1}, \forall s \geq 0. \quad \text{eq:hats_def2} \quad (76)$$

Next, we have

$$\frac{t_{N_s}^s}{\sigma_{N_s}^s} \stackrel{(a)}{=} \frac{t_0^{s+1}}{\sigma_0^{s+1}}, \quad t_{N_s}^s \stackrel{(b)}{\geq} t_0^{s+1} \stackrel{(c)}{=} t_0^{s+1} \theta_0^{s+1}, \quad \text{eq:switch_01} \quad (77)$$

$$t_{N_s}^s \sigma_{N_s}^s \stackrel{(b)}{\geq} t_0^{s+1} \sigma_0^{s+1} \stackrel{(c)}{=} t_0^{s+1} \sigma_0^{s+1} \theta_0^{s+1}, \quad \text{eq:switch_03} \quad (78)$$

where (a) follows from the definition of $t_k^s = \frac{\sigma_k^s}{\sigma_0^s}$, (b) holds by $\{t_k^s, \sigma_k^s\}$ is an increasing sequence in k , and (c) holds by $\theta_0^{s+1} = 1$. Hence, it follows from (76), (77) and (78) that

$$\begin{aligned} & t_{N_s}^s \left(\frac{(\tau_{N_s}^s)^{-1}}{2} \|\mathbf{x}^* - \mathbf{x}_0^{s+1}\|^2 + \frac{1}{2\sigma_{N_s}^s} \|\tilde{\mathbf{y}}^* - \mathbf{y}_0^{s+1}\|^2 \right. \\ & \quad \left. + \langle G(\mathbf{x}_0^{s+1}) - G(\mathbf{x}_{N_s}^s), \mathbf{y}_0^{s+1} - \tilde{\mathbf{y}}^* \rangle + \frac{1}{2\delta/\sigma_{N_s}^s} \|G(\mathbf{x}_0^{s+1}) - G(\mathbf{x}_{N_s}^s)\|^2 \right) \\ \geq & t_0^{s+1} \left(\frac{(\tau_0^{s+1})^{-1} - \rho_0^{s+1}}{2} \|\mathbf{x}^* - \mathbf{x}_0^{s+1}\|^2 + \frac{1}{2\sigma_0^{s+1}} \|\mathbf{y}^* - \mathbf{y}_0^{s+1}\|^2 \right. \\ & \quad \left. + \theta_0^{s+1} \langle \mathbf{y}_0^{s+1} - \tilde{\mathbf{y}}^*, G(\mathbf{x}_0^{s+1}) - G(\mathbf{x}_{N_s}^s) \rangle + \frac{\theta_0^{s+1}}{2\delta/\sigma_0^{s+1}} \|G(\mathbf{x}_0^{s+1}) - G(\mathbf{x}_{N_s}^s)\|^2 \right) \\ = & t_{j+1} Q_{j+1}(\mathbf{x}^*, \tilde{\mathbf{y}}^*), \end{aligned} \quad \text{eq:mid_res_lem_03} \quad (79)$$

where j corresponds to (s, N_s) . Then we complete the proof of (74) by putting (75) and (79) together.

Now, placing $(\mathbf{x}, \mathbf{y}) = (\mathbf{x}^*, \tilde{\mathbf{y}}^*)$, $(\mathbf{x}_{k+1}, \mathbf{y}_{k+1}) = (\mathbf{x}_{j+1}, \mathbf{y}_{j+1})$ in (54) and multiplying t_j on both sides, we have

$$\begin{aligned} 0 & \leq t_j [\mathcal{L}(\mathbf{x}_{j+1}, \tilde{\mathbf{y}}^*) - \mathcal{L}(\mathbf{x}^*, \mathbf{y}_{j+1})] \\ & \leq t_j \left[\frac{\tau_j^{-1} - \rho_j}{2} \|\mathbf{x} - \mathbf{x}_j\|^2 - \frac{\tau_j^{-1}}{2} \|\mathbf{x} - \mathbf{x}_{j+1}\|^2 + \frac{\theta_j}{2\delta/\sigma_{j-1}} \|\mathbf{q}_j\|^2 - \frac{1}{2\delta/\sigma_j} \|\mathbf{q}_{j+1}\|^2 \right. \\ & \quad \left. + \frac{1}{2\sigma_j} (\|\mathbf{y} - \mathbf{y}_j\|^2 - \|\mathbf{y} - \mathbf{y}_{j+1}\|^2) + \langle \mathbf{y} - \mathbf{y}_{j+1}, \mathbf{q}_{j+1} \rangle - \theta_j \langle \mathbf{y} - \mathbf{y}_j, \mathbf{q}_j \rangle \right. \\ & \quad \left. - \frac{\sigma_j^{-1} - \theta_j \delta / \sigma_{j-1}}{2} \|\mathbf{y}_{j+1} - \mathbf{y}_j\|^2 + \frac{L_G^2}{2\delta/\sigma_j} \|\mathbf{x}_{j+1} - \mathbf{x}_j\|^2 - \frac{\tau_j^{-1} - L_{XY}}{2} \|\mathbf{x}_{j+1} - \mathbf{x}_j\|^2 \right] \\ & \stackrel{(a)}{\leq} t_j Q_j(\mathbf{x}^*, \tilde{\mathbf{y}}^*) - t_{j+1} Q_{j+1}(\mathbf{x}^*, \tilde{\mathbf{y}}^*) - \nu_1 t_j \left[\frac{1}{2\tau_j} \|\mathbf{x}_{j+1} - \mathbf{x}_j\|^2 + \frac{1}{2\sigma_j} \|\mathbf{y}_{j+1} - \mathbf{y}_j\|^2 \right], \end{aligned} \quad \text{eq:res_01} \quad (80)$$

where (a) following (74) and (64). It follows from (65) and $\langle \mathbf{y}_j - \tilde{\mathbf{y}}^*, \mathbf{q}_j \rangle \geq -\frac{1}{2\delta/\sigma_{j-1}} \|\mathbf{q}_j\|^2 - \frac{\delta/\sigma_{j-1}}{2} \|\tilde{\mathbf{y}}^* - \mathbf{y}_k\|^2$ that

$$\begin{aligned} t_j Q_j(\mathbf{x}^*, \tilde{\mathbf{y}}^*) & \geq t_j \left(\frac{1}{2\tau_j} \|\mathbf{x}^* - \mathbf{x}_j\|^2 + \frac{1}{2\sigma_j} \|\tilde{\mathbf{y}}^* - \mathbf{y}_j\|^2 - \frac{\theta_j \delta}{2\sigma_{j-1}} \|\mathbf{y}_j - \tilde{\mathbf{y}}^*\|^2 \right) \\ & \stackrel{(a)}{\geq} t_j \left(\frac{1}{2\tau_j} \|\mathbf{x}^* - \mathbf{x}_j\|^2 + \frac{1}{2\sigma_j} \|\tilde{\mathbf{y}}^* - \mathbf{y}_j\|^2 - \frac{\delta}{2\sigma_{j-1}} \|\mathbf{y}_j - \tilde{\mathbf{y}}^*\|^2 \right) \\ & \geq \nu_2 \left(\frac{1}{2} \|\mathbf{x}^* - \mathbf{x}_k\|^2 + \frac{1}{2} \|\mathbf{y}_k - \tilde{\mathbf{y}}^*\|^2 \right) > 0, \end{aligned} \quad \text{eq:res_02} \quad (81)$$

where (a) holds by $\theta_j \leq 1$. By combining (80) and (81), we complete our proof of (66). \square

C.2 Proof of Theorem 3

Proof. Since $(\mathbf{x}_j, \mathbf{y}_j) \in \mathcal{X} \times \mathcal{Y}$ is a bounded sequence, it must have a convergent subsequence $\lim_{n \rightarrow \infty} (\mathbf{x}_{j_n}, \mathbf{y}_{j_n}) = (\mathbf{x}^*, \mathbf{y}^*)$, where \mathbf{y}^* is the limit point. We claim that limit point $(\mathbf{x}^*, \mathbf{y}^*)$ satisfies the KKT condition. Placing $a_j = t_j Q_j(\mathbf{x}^*, \tilde{\mathbf{y}}^*)$, $b_j = \nu_1 t_j \left[\frac{1}{2\tau_j} \|\mathbf{x}_{j+1} - \mathbf{x}_j\|^2 + \frac{1}{2\sigma_j} \|\mathbf{y}_{j+1} - \mathbf{y}_j\|^2 \right]$ and $c_j = 0$ in Lemma 5. It follows from (66) in Lemma 2 that $a_j \geq 0, b_j > 0$. Hence, we have $\sum_{j=0}^{\infty} \|\mathbf{x}_{j+1} - \mathbf{x}_j\|^2 < \infty$, and $\sum_{j=0}^{\infty} \|\mathbf{y}_{j+1} - \mathbf{y}_j\|^2 < \infty$, which implies $\lim_{n \rightarrow \infty} \|\mathbf{x}_{j_n} - \mathbf{x}_{j_n+1}\|^2 = 0$ and $\lim_{n \rightarrow \infty} \|\mathbf{y}_{j_n} - \mathbf{y}_{j_n+1}\|^2 = 0$.

Hence, according to the first-order optimality condition, we have

$$\mathbf{0} \in \partial f(\mathbf{x}^*) + \nabla G(\mathbf{x}^*)\mathbf{y}^* + \mathcal{N}_{\mathcal{X}}(\mathbf{x}^*). \quad \text{eq:mid-opt-01} \tag{82}$$

Next, we show the complementary slackness holds for $(\mathbf{x}^*, \mathbf{y}^*)$. , we have

$$0 \leq -\langle G(\mathbf{x}^*), \mathbf{y}^* \rangle \leq -\langle G(\mathbf{x}^*), \mathbf{y} \rangle, \quad \forall \mathbf{y} \in \mathcal{Y}.$$

Moreover, due to the complementary slackness, there exists an $\hat{\mathbf{y}}^* \in \mathcal{Y}^* \subseteq \mathcal{Y}$ such that $-\langle G(\mathbf{x}^*), \hat{\mathbf{y}}^* \rangle = 0$. Hence, we must have $\langle G(\mathbf{x}^*), \mathbf{y}^* \rangle = 0$, which, together with (82), implies that $(\mathbf{x}^*, \mathbf{y}^*)$ is KKT point. \square

D Proof Details in Section 5

The main proof is based on the modification of Section 4.2.3 in [17].

D.1 Proof of Theorem 4

Proof. The step-size $\tau_k^s = \tau_0^s, \sigma_k^s = \sigma_0^s$ are unchanged at one epoch, which implies that $\rho_{k+1} = 0$ in (15), i.e., (19) and (20) are satisfied. By the definition of τ_0^s and σ_0^s , we have

$$(\tau_0^s)^{-1} = L_{XY} + \frac{L_G^2 \tilde{\sigma}}{\delta} 2^{\frac{s}{2}} = L_{XY} + \frac{L_G^2 \sigma_0^s}{\delta}$$

which means equality holds at the first term in (18).

Since $g_i(\mathbf{x})$ is a strongly convex function with modulus μ_i , then we have

$$\begin{aligned} \mathcal{L}(\bar{\mathbf{x}}_K, \mathbf{y}^*) &\geq \mathcal{L}(\mathbf{x}^*, \mathbf{y}^*) + \frac{(\mathbf{y}^*)^T \boldsymbol{\mu}}{2} \|\bar{\mathbf{x}}_K - \mathbf{x}^*\|^2, \\ \mathcal{L}(\mathbf{x}^*, \mathbf{y}^*) &\geq \mathcal{L}(\mathbf{x}^*, \bar{\mathbf{y}}_K). \end{aligned}$$

Summing up the two inequalities above, we can get

$$\mathcal{L}(\bar{\mathbf{x}}_K, \mathbf{y}^*) - \mathcal{L}(\mathbf{x}^*, \bar{\mathbf{y}}_K) \geq \frac{(\mathbf{y}^*)^T \boldsymbol{\mu}}{2} \|\bar{\mathbf{x}}_K - \mathbf{x}^*\|^2. \quad \text{eq:12-1-1} \tag{83}$$

Combining (36) and (83), we can obtain (37). \square

E Proof Details in Section 6

E.1 Proof of Lemma 3

Proof. It follows from (57) that $\|\mathbf{x}_1^s - \mathbf{x}^*\| \leq \sqrt{\frac{\sigma_0^s \tau_0^s}{\sigma_1^s} (\frac{1}{\tau_0^s} \|\mathbf{x}_0^s - \mathbf{x}^*\|^2 + \frac{1}{\sigma_0^s} \|\mathbf{y}_0^s - \mathbf{y}^*\|^2)}$. Hence, in order to prove $\|\mathbf{x}_1^s - \mathbf{x}^*\| \leq \frac{\eta}{3L_{XY}} \frac{\tau_k^s}{\tau_k^s + (2L_{XY})^{-1}}$, we need to prove

$$\sqrt{\frac{\sigma_0^s \tau_0^s}{\sigma_1^s} (\frac{1}{\tau_0^s} \|\mathbf{x}_0^s - \mathbf{x}^*\|^2 + \frac{1}{\sigma_0^s} \|\mathbf{y}_0^s - \mathbf{y}^*\|^2)} \leq \frac{\eta}{3L_{XY}} \frac{\tau_1^s}{\tau_1^s + (2L_{XY})^{-1}} \quad \text{eq:suff_cond-1} \tag{84}$$

From Corollary 1 and Theorem 2, 3, we know that the left hand side of (84) converges to 0 and right hand side of (84) is a positive constant. Hence, there exist a \hat{S}_2 such that (84) holds, which implies (42) holds for $k = 1, s = \hat{S}_2$. Now we use induction to prove

$$\sqrt{\frac{\sigma_0^{\hat{S}_2} \tau_k^{\hat{S}_2}}{\sigma_k^{\hat{S}_2}} (\frac{1}{\tau_0^{\hat{S}_2}} \|\mathbf{x}_0^{\hat{S}_2} - \mathbf{x}^*\|^2 + \frac{1}{\sigma_0^{\hat{S}_2}} \|\mathbf{y}_0^{\hat{S}_2} - \mathbf{y}^*\|^2)} \leq \frac{\eta}{3L_{XY}} \frac{\tau_k^{\hat{S}_2}}{\tau_k^{\hat{S}_2} + (2L_{XY})^{-1}}, \forall k \in [N_{\hat{S}_2}]. \quad \mathbf{x_small_k-1} \tag{85}$$

When $k = 1$, inequality (85) coincides with (84) with $s = \hat{S}_2$. Now, assume (85) holds for k , we aim to prove (85) holds for $k + 1$. It follows from (57) that

$$\begin{aligned}
& \|\mathbf{x}_{k+1}^{\hat{S}_2} - \mathbf{x}^*\| \\
& \leq \sqrt{\frac{\sigma_0^{\hat{S}_2} \tau_{k+1}^{\hat{S}_2}}{\sigma_{k+1}^{\hat{S}_2}} \left(\frac{1}{\tau_0^{\hat{S}_2}} \|\mathbf{x}_0^{\hat{S}_2} - \mathbf{x}^*\|^2 + \frac{1}{\sigma_0^{\hat{S}_2}} \|\mathbf{y}_0^{\hat{S}_2} - \mathbf{y}^*\|^2 \right)} \\
& \stackrel{(a)}{\leq} \sqrt{\frac{\tau_{k+1}^{\hat{S}_2}}{\sigma_{k+1}^{\hat{S}_2}} \cdot \frac{\sigma_k^{\hat{S}_2}}{\tau_k^{\hat{S}_2}} \cdot \frac{\eta}{3L_{XY}} \cdot \frac{\tau_k^{\hat{S}_2}}{\tau_k^{\hat{S}_2} + (2L_{XY})^{-1}}} \\
& = \sqrt{\frac{\sigma_k^{\hat{S}_2}}{\sigma_{k+1}^{\hat{S}_2}} \cdot \frac{\tau_k^{\hat{S}_2}}{\tau_{k+1}^{\hat{S}_2}} \cdot \frac{\eta}{3L_{XY}} \cdot \frac{\tau_{k+1}^{\hat{S}_2}}{\tau_k^{\hat{S}_2} + (2L_{XY})^{-1}}} \\
& \stackrel{(b)}{=} \frac{\eta}{3L_{XY}} \cdot \frac{\tau_{k+1}^{\hat{S}_2}}{\tau_k^{\hat{S}_2} + (2L_{XY})^{-1}} \\
& \stackrel{(c)}{\leq} \frac{\eta}{3L_{XY}} \cdot \frac{\tau_{k+1}^{\hat{S}_2}}{\tau_{k+1}^{\hat{S}_2} + (2L_{XY})^{-1}},
\end{aligned}$$

where (a) follows from induction, (b) holds by $\frac{\tau_k^{\hat{S}_2}}{\tau_{k+1}^{\hat{S}_2}} = \sqrt{\frac{\gamma_{k+1}^{\hat{S}_2}}{\gamma_k^{\hat{S}_2}}}$ and $\frac{\sigma_k^{\hat{S}_2}}{\sigma_{k+1}^{\hat{S}_2}} = \frac{\gamma_k^{\hat{S}_2} \tau_k^{\hat{S}_2}}{\gamma_{k+1}^{\hat{S}_2} \tau_{k+1}^{\hat{S}_2}} = \sqrt{\frac{\gamma_k^{\hat{S}_2}}{\gamma_{k+1}^{\hat{S}_2}}}$ deduced by (19)

and (20), and (c) holds by $\tau_{k+1}^{\hat{S}_2} \leq \tau_k^{\hat{S}_2}$. Hence, we complete our proof of (85).

From Theorem 2, we have $\|\mathbf{x}_0^s - \mathbf{x}^*\|^2 \leq D_X^2 \cdot 2^{-s}$. Hence, there exists a $\hat{S}_3 = \lceil 2 \log_2 \{ D_X (\frac{\eta}{3L_{XY}} \frac{\bar{\tau}}{\bar{\tau} + (2L_{XY})^{-1}})^{-1} \} \rceil$ such that $\|\mathbf{x}_0^{\hat{S}_3} - \mathbf{x}^*\| \leq D_X \cdot 2^{-\hat{S}_3/2} \leq \frac{\eta}{3L_{XY}} \frac{\bar{\tau}}{\bar{\tau} + (2L_{XY})^{-1}}$, which implies that $\|\mathbf{x}_0^s - \mathbf{x}^*\| \leq D_X^2 \cdot 2^{-s} \leq \frac{\eta}{3L_{XY}} \frac{\bar{\tau}}{\bar{\tau} + (2L_{XY})^{-1}}$ holds for any $s \geq \hat{S}_3$.

It follows from the definition of \hat{S}_1 in (41) and step-sizes will be reset at different epoch, then we have (84) holds for $s \geq \max\{\hat{S}_1, \hat{S}_2\}$, which implies that (85) holds with substituting \hat{S}_2 as any $s \geq \max\{\hat{S}_1, \hat{S}_2\}$. Hence, we can obtain that there exist a $\hat{S}_0 = \max\{\hat{S}_1, \hat{S}_2, \hat{S}_3\}$ such that (42) holds. \square